Title
Assessing the Performance of Vadose Zone Monitoring Systems using Bromide as a Tracer

Author
Lennon, William

Publication Date
2024

Peer reviewed|Thesis/dissertation

Assessing the Performance of Vadose Zone Monitoring Systems using Bromide as a Tracer

By

WILLIAM NICOLAS LENNON
THESIS

Submitted in partial satisfaction of the requirements for the degree of

MASTER OF SCIENCE

in

Hydrologic Sciences

in the

OFFICE OF GRADUATE STUDIES

of the

UNIVERSITY OF CALIFORNIA

DAVIS

Approved:

____

Isaya Kisekka

____

Thomas Harter

____

Helen Dahlke

Committee in Charge

2023

TABLE OF CONTENTS

LIST OF FIGURES 4

LIST OF TABLES 5

LIST OF EQUATIONS 5

Abstract 6

Chapter 1: Review of Literature and Rationale 8

Groundwater Contamination 8

Vadose zone 10

Nitrate Leaching Monitoring Techniques 11

Nitrate Leaching Modeling Tools 15

Temperature as a tracer 18

Bromide as a tracer 19

Objective of study 20

Chapter 2: Vadose Monitoring System Assessment 21

Materials and Methods 21

1. Study areas and measurement periods 21

2. HYDRUS 1D Model Inputs 29

3. Tracer Application and Treatments: 32

4. Bromide Analysis: Ion Selective Electrode 34

5. Change in Bromide Soil Storage Computation 36

Results 37

1. Site 1: Esparto 37

2. Site 2: Bowman 41

3. Site 3: Booth Ranch 47

Discussion 52

Chapter 3: Conclusions and Future Work 55

References 57

ACKNOWLEDGMENTS

There are many people who I owe debt of gratitude in completing this thesis. First I would like to thank Professor Isaya Kisekka for overseeing the project and whose advice was essential to the entirety of the study. I thank Professor Thomas Harter for being a mentor throughout the duration of my graduate studies. I also thank Helen Dahkle for contributing supplies and wisdom to the tracer experiment as well as serving on my thesis committee. Iael Hoffman and Felix Ogunmokun were both vital in the experimental design and formulation of my thesis. I extend my gratitude to Nicolas Almeida, Spencer Jordan and Floyid Nicolas for their collaboration throughout this project.

Finally, I would like to thank my parents, Ronnie and Carrie Lennon. Their love and support throughout my life has inspired me to become the researcher I am today.

This work is dedicated to my grandfather, Thornton Jenkins who always encouraged me to pursue a degree in higher education.

This study was supported by the USDA NRCS grant number NR193A750023C016, and USDA NIFA Award number 2021-68012-35914.

LIST OF FIGURES

Figure 1. Diagram of soil profile highlighting important hydrological processes within the vadose zone. 10

Figure 2. Schematic of a Vadose Zone Monitoring System. 21

Figure 3. Map Study Sites. 21

Figure 4. Soil texture classes for the Esparto site near Esparto, CA. 24

Figure 5. Large cracks observed in the field. 24

Figure 6. Soil texture classes for the Bowman Orchard near Modesto, CA.. 27

Figure 7. Soil texture class for Booth Ranch site near Orange Cove, CA. 28

Figure 8. Tracer application system 33

Figure 9. Thermo Scientific™ Bromide ionplus® Sure-Flow® Solid State Combination Ion Selective Electrode. 36

Figure 10. Esparto VMS measured water content (upper) and temperature (lower) 38

Figure 11. Esparto observed and simulated bromide concentrations. 40

Figure 12. Bowman VMS measured water content (upper) and temperature (lower) 43

Figure 13. Bowman observed and simulated bromide concentrations 46

Figure 14. Booth VMS measured water content (upper) and temperature (lower) 51

Figure 15. Booth observed and simulated bromide concentrations 51

LIST OF TABLES

Table 1. Esparto Vadose Sampling Port (VSP) depth and corresponding soil texture. 22

Table 2. Bowman orchard near Modesto CA, Vadose Sampling Port (VSP) depths and corresponding soil textures. 25

Table 3. Booth ranch near Orange Cove, CA Vadose Sampling Port (VSP) depths and corresponding soil textures. 27

Table 4. Esparto field site Soil Hydraulic Properties.. 29

Table 5. Bowman orchard Soil Hydraulic Properties.. 30

Table 6. Booth ranch Soil Hydraulic Properties 30

Table 8. Site based treatment, study period, and facilitated flow.. 34

Table 9. Change in Esparto soil bromide concentration from the start to the end of the study period at each VSP. 41

Table 10. Change in Bowman soil bromide storage from the start to the end of the study period at each VSP. 46

Table 11. Change in Bowman soil bromide storage from the start to the end of the study period at each VSP. 51

LIST OF EQUATIONS

Equation 1: Modified Richard's Equation. 17

Equation 2. van Genuchten-Mualem Equation... 17

Equation 3. Convection Dispersion Equation.. 18

Equation 4. Nernst Equation.. 34

Equation 5. Change in soil bromide storage. 36

Abstract

Understanding the fate and transport of nitrogen through the vadose zone is vital to reduce nitrate leaching, protecting groundwater quality, and enhancing resource use efficiency. Currently, there is limited data on the continuous monitoring of nitrate transport through the deep vadose zone. The lack of high-quality data makes it difficult to evaluate the effectiveness of conservation practices aimed at reducing nitrate leaching. The vadose-zone monitoring system (VMS) serves as an innovative technology for near real-time monitoring of nitrate and other contaminants as they travel through the shallow and deep vadose zone to groundwater. The objective of this study was to evaluate the performance of the VMS technology at three sites using bromide (Br^-) as a tracer and the unsaturated flow model HYDRUS 1D to understand underlying vadose zone water flow and solute transport processes. Site 1 was a field crop site near Esparto, CA, with a heavy Capay-clay soil and a groundwater depth of approximately 10 m. Site 2 was an almond orchard near Modesto, CA, with a moderately homogenous sandy loam in the top 2 m and a sandy clay loam down to 6 m and a water table at approximately 8 m. Site 3 was a citrus orchard near Orange Cove, CA, with a sandy loam soil at the shallow depths (0-2 meters) followed by sandy clay loam down to 7 m and a groundwater depth of approximately 25 m. The VMS was installed at all sites to collect soil pore water samples at approximately 1 m intervals to about 7 m depth. To test the system performance, approximately 380 L of a 500 ppm Br^- solution was applied as a conservative tracer at the three sites. The applied tracer was either percolated by rain, irrigation, or a combination of the two. The site HYDRUS models demonstrated a complete breakthrough of Br^- at each vadose sampling port depth. Measured pore-water from the VMS exhibited similar solute breakthroughs with varying time and concentrations. The bromide tracer results confirm that the VMS is capable of monitoring flow and transport processes in the deep vadose zone.

Chapter 1: Review of Literature and Rationale

Groundwater Contamination

The contamination of subsurface sources of water is a global issue. More than a third of the world's population depends on groundwater for drinking (International Association of Hydrogeologists, 2023). Groundwater is significantly important to communities living in arid and semi-arid regions (Venkatesan et al., 2021). Climate change and land development have caused a shift in the dependance on different sources for freshwater.

Large-scale agriculture in California's Central Valley has experienced a revolution in both irrigation and crop management. Intensive farming has created a plethora of environmental issues. Crop production significantly increases when nitrate is imputed into a system (Delgado, 2002). Applications that exceed nitrogen plant root uptake leach through the soil profile into the groundwater via irrigation or precipitation. Nitrate-nitrogen has been identified as the most common pollutant observed in the Central Valley aquifer system (Harter et al. 2017). Consumption of nitrate at levels higher than 10 mg N/L can lead to serious health implications (Jordan and Weller, 1996). These issues include nausea, methemoglobinemia, and various cancers. The constituent is an important parameter in groundwater pollution assessment and used as an indicator for vulnerability of contamination (Evans 1995). Surface waters are also susceptible to nitrogen loading from groundwater contributions. The subsurface flows can leach into lakes or ponds that can then become a sink for nutrients. These sinks can become an issue due to eutrophication and the succession of large blooms of algae and noxious aquatic plants like Eurasian Millfoil.

Whether forced by regulatory agencies, or an effort to reduce costs, or use of other finite resources, farmers have developed practices that can maximize efficiency through precision farming. The protection of groundwater resources has become paramount for the future of the sustainability of agriculture. Grower accountability for groundwater contamination has promoted the passage of Central Valley Salinity Alternatives for Long-Term Sustainability (CV-SALTS) and Irrigated Lands Regulatory Program (IRLP). Using subsurface drip irrigation methods and other micro-irrigation technologies not only reduces evaporation losses and over-watering, but enables farmers to directly inject required quantities of fertilizer with the irrigation water as needed by the crop, a process known as fertigation. Understanding the movement of fertilizers throughout the soil profile is key to recognizing when and how it might reach the groundwater.

The complexity of the soil-water interface and percolation creates ambiguity in understanding anthropogenic effects on groundwater quality. Percolation and contaminant transport are typically modeled using estimates of hydraulic parameters and numerical solutions (Rimon 2007). Numerical models are often informed by field-measured data, however, field measurements of soil water content and nitrate concentrations is often limited to few samples that can fail to capture the dynamic processes that occur in the rootzone such as variably saturated flow and transport. Developing a methodology that produces repeatable and accurate data is an integral step in recognizing the time lag between the initial introduction of the contaminant injection and its detection in groundwater. The use of suction lysimeters is one of the most common methods used to monitor nitrate transport through a soil column (Pampolino et al. 2000). Historically, agri-environmental methods such as tracking a nitrogen balance were used to predict the leaching of nitrate into groundwater (Wick et al. 2012). When used alone, the mass balance approach cannot capture the different degrees of complexity that occur in the plant-fertilizer-water-soil matrix. In addition to these uncertainties in obtaining field data, constituents within the unsaturated are incredibly difficult to model due to the heterogeneity of soils and their influence on transport processes (Almarsi, 2007).

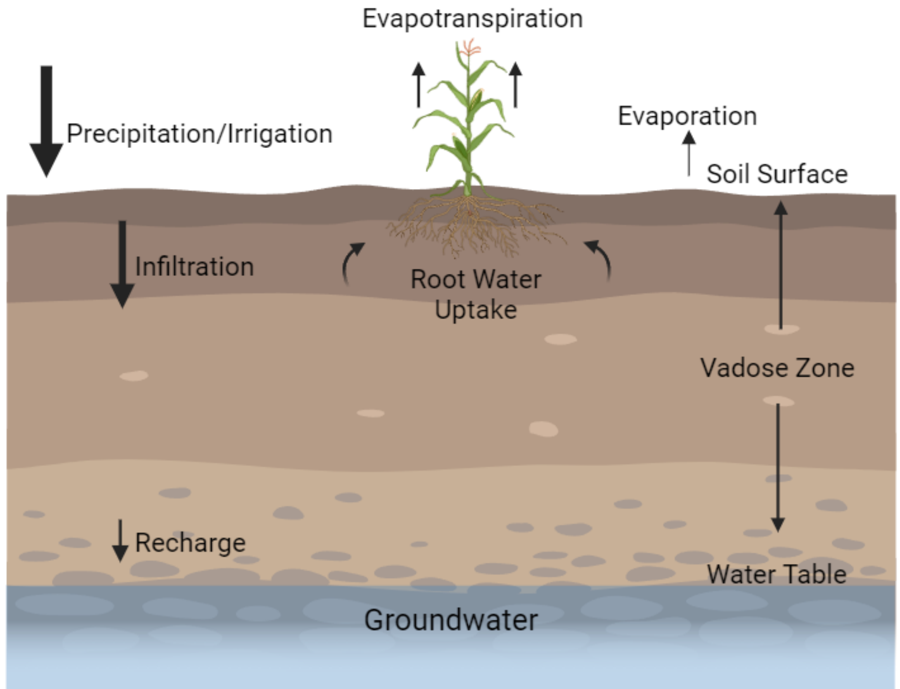

Figure 1. *Diagram of soil profile highlighting important hydrological processes within the vadose zone.*

Vadose zone

The vadose zone (also known as the unsaturated or variably saturated zone) is the extent of the soil profile from the surface to the regional ground water table (Holden et al. 2005). Depending on the depth to groundwater, the unsaturated zone can range from a few to hundreds of meters. Water quality in the vadose zone is influenced by climate, vegetation, and geology but also management practices occurring on the land surface, which largely influence the leaching potential of contaminants through the soil profile. Soil water can drastically change the chemistry of surface and subsurface waters, making it a subject of a variety of research projects (Singh et al., 2017). The fate of chemicals and contaminants in the unsaturated zone is of interest to both crop management and evaluating environmental risks (Aharoni et al., 2017). The dissolved solutes in soil water are available to plants, therefor their concentration is important to nutrient assimilation (Raij-Hoffman et al., 2020). Vadose monitoring is beneficial because it can potentially serve as an early warning for groundwater contamination from hazardous constituents (U.S. EPA, 1978). This warning can indicate when action and remediation is necessary on the overlying surface (Durant et al., 1993).

Nitrate Leaching Monitoring Techniques

There are a variety of tools to help managers and researchers recognize the potential for contaminant transport through the unsaturated zone and into groundwater. Sampling devices are chosen based on the research objective, financial resources, and/or characteristics of the research site (Brandi-Dohrn et al., 1996). However, each approach has its advantages and disadvantages as outlined below.

Soil Coring

Soil coring is one of the oldest methods for monitoring constituents in the subsurface. The financial requirement is quite low, and procedures are straightforward and transparent. Soil coring has its limitations however as it is a destructive method to sample chemical composition. It cannot be replicated in the same location without interfering with soil hydraulic properties and requires a high sampling frequency to monitor changes over time.

Ion Exchange Resin Bags

Ion exchange bags use anion and cation beads that absorb ions from the pore water solution as it percolates through the soil profile. Low costs of fabrication and ease of installation make them popular in studying long term changes in soil chemistry (Singh, et al. 2017). The duration of the monitoring period and placement of the bags can however create inconsistencies in detecting fluxes through the soil, which is the reason why these bags are typically considered as an unreliable tool for measuring nutrient flows (Sherrod et al., 2002).

Suction Lysimeters

The use of suction lysimeters is one the most common methods to analyze/quantify nitrate transport through a soil column (Pampolino et al. 2000). Low suction is applied within the suction lysimeter to create a negative pressure that pulls the soil-pore water solution through a porous cup made of ceramic, stainless steel or quartz into a reservoir in the suction cup. The solution concentration of pore water is analyzed to establish constituents fluxes at varying depths. Lysimeters allow sampling the same location over multiple, consecutive sampling events, however the exact source of the leachate is harder to differentiate due to the nature of the soils and flow patterns (Weihermuller et al., 2005). Spatial and temporal variability can be accounted for by installing a large number of suction cups. Preferential flow paths along the extent of the lysismeter's tubing can create inaccuracies in measuring concentrations at different depths of the soil. Independent soil water fluxes must be estimated when using tensiometers above and below the suction cups which creates further uncertainty when calculating solute fluxes (Weihermuller et. al., 2007).

The Vadose Zone Monitoring System

The Vadose Zone Monitoring System (VMS) is a plastic sleeve installed within the soil profile containing vadose sampling ports (VSP) and Time Domain Transmissometry (TDT) soil water content sensors set at defined intervals along the length of the sleeve (***figure 2***).

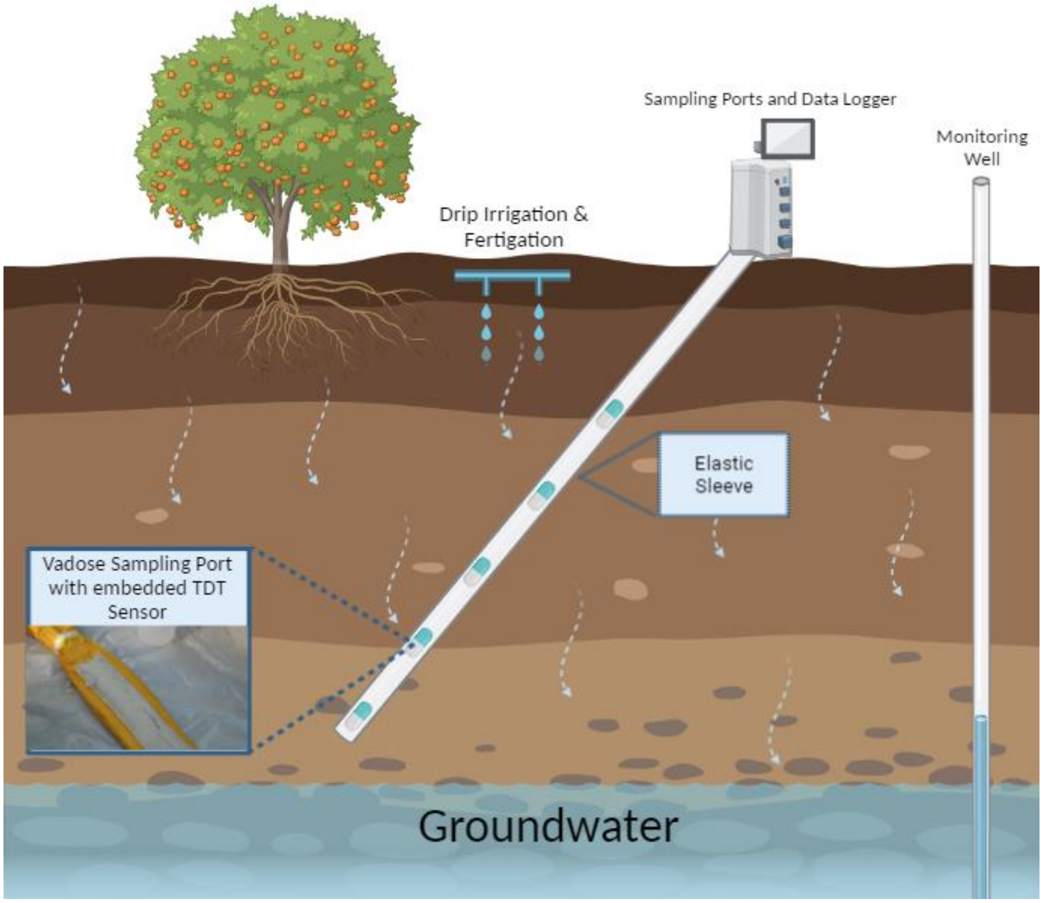

Figure 2. *Schematic of a Vadose Zone Monitoring System.*

The VSP is composed of a large suction cup surrounded by fine porous medium (e.g., glass beads) in which, under vacuum, a solution is extracted from the pore space of the soil. The sleeve sits in a borehole that was drilled at 45^{o} to the vertical to ensure that the profile of the overlying soil is not disturbed during installation, limiting the potential for preferential flow paths (Dahan et al. 2009). Upon fitting the sleeve into the borehole, it is filled with grout to rebuild the hydraulic pressure of soil and to avoid preferential flows caused by voids in between the soil and the sleeve. This process also ensures adequate contact between the VSP and the soil. Through the TDT sensors, the VMS continuously monitors the moisture content of the soil. Sample and data collection is completed entirely in one control panel. A series of stainless steel pressure manifolds and sampling ports are located within the panel, along with a Campbell Scientific CR1000X data logger connected to a satellite antenna for remote data telemetry A 30 watt solar panel supplies the charge to a 12V sealed battery which, in turns, delivers power to the entire system.

Due to the nature of the system installation, any issues (sensor failure, severance in sampling line, etc.) within the sleeve are irreparable. Once completed, none of the individual measurement tools, including their access and transmission lines can be accessed or repaired without effectively destroying the VMS. Preferential flow paths along the sleeve itself may be a source of error for soil water solution sampling. As of 2019, a single VMS costs roughly $85,000 for the entire system and sleeve. The drilling crew and equipment necessary for installation approximately costs $5,000 per system.

The VMS was developed for real-time monitoring of water and contaminant transport through the vadose zone (Dahan et al. 2009). The slanted installation ensures each VSP is located under its own undisturbed column of soil and the integrated data from the VMS can be representative for a wider zone rather than a single vertical profile (Turkeltaub et al., 2016). The sloped borehole voids the destruction of the natural soil properties above each sensor that a vertical borehole may create. This disturbance can create preferential flow paths through the backfilled material as well as a reduction of lithostatic pressure (Dahan et al., 2003).

Observation Well

Monitoring wells also known as observation wells are the standard regulatory and scientific tool to detect constituents found in groundwater. Monitoring wells serve as an observation point to measure groundwater levels and provide samples that accurately represent aquifer water conditions at the particular sampling time (Aller et al., 1991). Wells aid in the detection of harmful contaminants as well as the changes from pumping and recharge. Proper installation of observation wells is vital to ensure accuracy and integrity of the samples provided. If well design and construction is flawed, data collected may be unreliable and inaccurate (Sosebee et al., 1983). Improper sealing methods can introduce vertical seepage and flow paths along well casing (Environmental Protection Agency, 1986). Monitoring wells are limited by the soils where they are placed and, alone, cannot be used to predict leaching on a field wide scale. Contaminants may not reach a monitoring well, even if completed immediately below the water table, for months or even years after contaminants have been released from the land surface or the root zone.

For management of land uses for groundwater protection, especially agricultural land uses, an earlier feedback and warning system than monitoring wells would provide important advantages (Harter et al., 2017).

Nitrate Leaching Modeling Tools

Modeling is an effective tool used to simulate and assess a wide variety of water resources issues at a range of scales. The ability for researchers, managers, and growers to perform large scale assessments has put modeling on the forefront of resource conservation and management. There is an assortment of modeling platforms that are popular across different agricultural and environmental disciplines.

<u>SWAT</u>

The Soil and Water Assessment Tool (SWAT) is a basin-scale, daily time step model that allows users to assess the impact of different management practices for a selected watershed

(Gassman et al., 2007). SWAT is a physically based model that uses soil properties, climate, hydrology, and land use/land cover data to estimate rainfall-runoff dynamics for different watershed properties. SWAT models have been applied in hundreds of studies across the world. While the model is discretized on the basis of hydrologic response units (HRUs), where each HRU represents a unique combination of soil, topography, and land use, SWAT may be inaccurate in predicting field scale and plot level processes. Model accuracy is contingent on the availability of sufficient monitoring data and scientific understanding of the watershed (Gassman et al., 2007). The SWAT model offers a variety of crop parameters and calibration is needed for accurate predictions of water and nutrient dynamics (Hoffman et al. 2022).

APEX

The Agricultural Policy/Environmental eXtender is a hydrologic model that assesses water quality, soil erosion and other environmental issues on a small farm or watershed scale (Gassman et al., 2005). APEX is capable of analyzing nutrient and sediment transport which aid in evaluating the conservation practices of agriculture (Francesconi. W., et al., 2014). Model calibration depends on adjustable field parameters and may result in large margins of error compared to the observed values.

DSSAT

Decision Support System for Agrotechnology Transfer (DSSAT) is a crop model used to understand the effects of land management decisions on production and the environment (Zamora et al., 2009). DSSAT uses crop simulation models based on soil science, meteorology, and crop physiology to compute processes such as leaching, runoff and organic matter decomposition (Jones et al., 2003). Soil water drainage is a function of the tipping bucket approach for layered soils and vertical movement is governed by the soil drainage factor

(Ritchie, 1998). DSSAT is more suitable for large landscape crop management and may be limited when assessing small scale contaminant transport (Hoogenboom et al., 2019).

<u>HYDRUS 1D</u>

HYDRUS-1D is a modeling environment based on Microsoft Windows software that allows for the analysis of water and solute transport through porous media under different conditions (Simunek et al., 2005). The program numerically simulates saturated and unsaturated water flow through porous media using Richards' equation.

Equation 1: *Modified Richard's Equation.*

$$\frac{\partial \theta}{\partial t} = \frac{\partial}{\partial x}\left[K\left(\frac{\partial h}{\partial x} + \cos a\right)\right] - S$$

Where h is the water pressure head (cm); θ is the volumetric water content; t is time; x is the spatial coordinate (positive upward); S is the sink term; α is the angle between the flow direction and the vertical axis; K is the unsaturated hydraulic conductivity function.

Changes in hydraulic conductivity with soil water content values are derived from the van Genuchten-Mualem equation.

Equation 2. *The van Genuchten-Mualem Equation.*

$$\theta(h) = \begin{cases} \theta_r + \dfrac{\theta_{s-}\theta_r}{[1 + |ah|^n]^m} & h \leq 0 \\ \theta_s & h > 0 \end{cases}$$

Where θ is volumetric water content at pressure head h; θ_S and θ_r are the saturated and residual soil water contents respectively; α is related to the inverse of air entry pressure; n is a measure of the pore size distribution; m = 1-1/n (van Genucten, 1980).

With respect to the solute transport, HYDRUS-1D uses advection-dispersion equations to solve for vertical, one-dimensional flow in an unsaturated porous media (Heatwole et al. 2007). Conservative, non-sorbing solute transport is solved numerically using the following equation:

Equation 3. *Convection Dispersion Equation.*

$$\frac{\partial(\theta C)}{\partial t} = \frac{\partial}{\partial z}\left(\theta D\frac{\partial C}{\partial z}\right) - \frac{\partial}{\partial z}(q_w C)$$

Where C is solute concentration (g/cm^3); θ is volumetric water content; D is the dispersion coefficient (cm^2/day); and q_w is the water flux (cm2/day).

Boundary conditions including drainage, surface runoff, and precipitation/irrigation can be calibrated for, influencing flow through a heterogeneous, site specific, soil profile. The model is one-dimensional. Therefore, it cannot account for lateral dispersion. Even though the VSPs are perpendicular to one another, for simplicity, the VSPs are treated as if they are vertically aligned for the HYDRUS simulation.

Vadose Zone Tracers

Temperature as a tracer

Heat transport has been used in groundwater tracer experiments as early as the 1960's (Anderson, 2005). Research using heat-tracing in the vadose zone is relatively new, but studies show that different temperature methods can be used to infer steady-state water flux in the unsaturated profile (Halloran et al. 2016). Utilization of heat-tracers requires knowledge of the thermal properties such as the heat capacity and conductivity of the parent material as well as the water saturation levels (Duque et al., 2015). These methods require a moderately wet and shallow soil profile as well as a large water flux to make accurate estimations in water movement. Temperature-based tracer experiments are limited to nearly saturated and/or coarse soils (Clutter, M. and Ferré, T.P.A., 2018).

Bromide as a tracer

There are a variety of acceptable ionic solutions used as tracers. Bromide (Br^-) is a conservative tracer that has been applied in many experiments to study leaching in the unsaturated zone (Bech et al., 2017). Low sorption rates, negligible background concentrations, low cost and ease of detection make Br^- suitable as well as popular when it comes to soil and groundwater tracer experiments (Davis, et al. 1980). In small-scale field studies, Br^- poses a low toxicity to most plants, freshwater organisms and mammals and little threat to biota (Fluryet al., 1993).

Objective of study

The overall objective of this study was to evaluate the capability of the VMS to monitor the transport of a constituent through the variably saturated zone.

This study aimed to achieve the following specific objectives:

1. Evaluate the ability of the VMS in measuring bromide as it is being transported through the soil profile.
2. Model each VMS as 1D soil column using HYDRUS 1D and compare simulated water flow and Br^- transport to field-observed data.
3. Use the concentration of Br^- in soil before tracer application and on final day of study period to demonstrate the change in storage.

Chapter 2: Vadose Monitoring System Assessment

Materials and Methods

1. *Study areas and measurement periods*

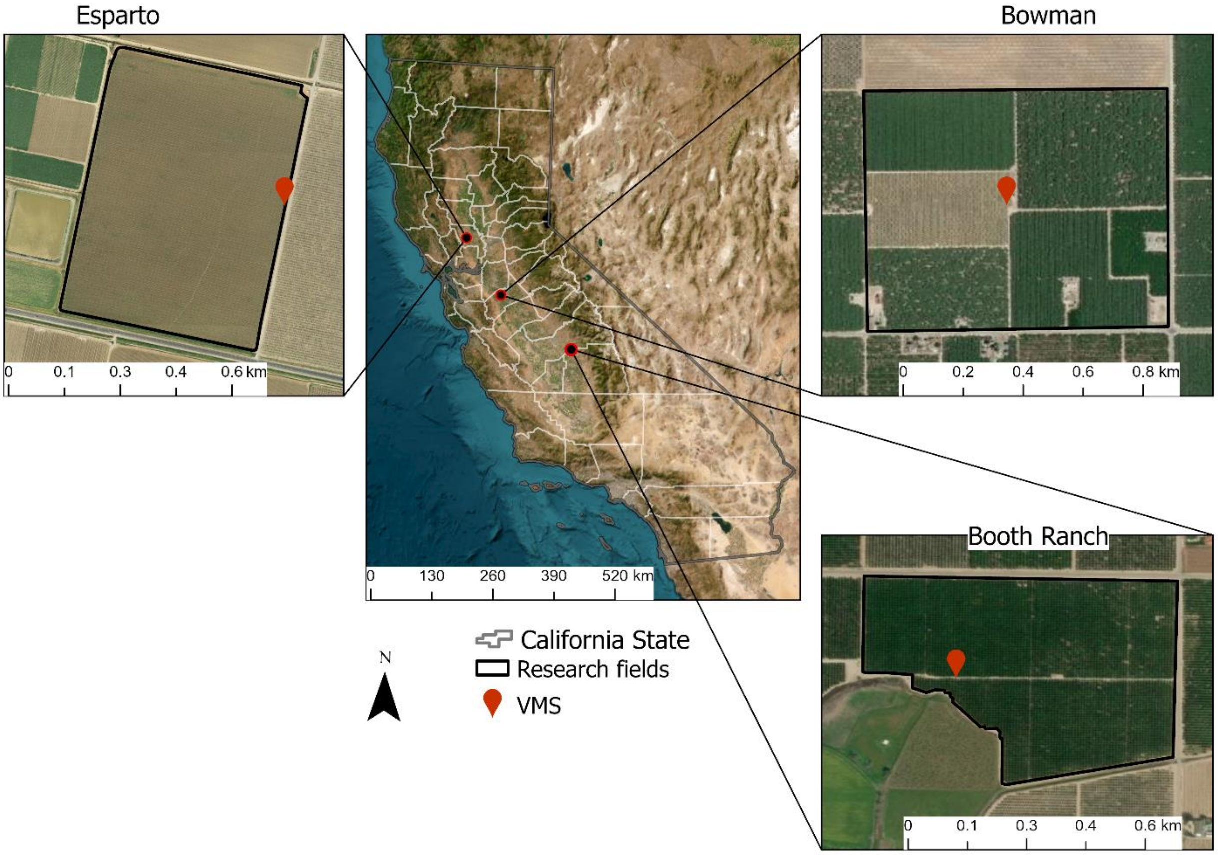

Figure 3. *Map of California counties bordered in black with inlay of the three study sites that form part of the Cal Vadose Zone Monitoring network. The Vadose Monitoring Systems (VMS) at each field are indicated with a red pin.*

Site 1: Tomato Rotation Field near Esparto, California.

The Esparto tomato field site is a 41 ha plot that rotates processing tomatoes with a seed or wheat crop (i.e., sunflower, cucumber, triticale) every other year. The grower uses subsurface drip irrigation and fertigation conservation practices at this site. Orchards, processing tomato and seed crops make up a majority of the bordering fields, with exception of a water treatment plant that is located to the west of the field site. The soil unit that makes up the majority of the site is a Capay silty clay derived from an alluvium material formed from igneous, metamorphic and sedimentary rock (USDA, 2023). The soil is classified as moderately well drained with high runoff potential and a tendency for frequent ponding under large precipitation events. Mean annual precipitation in the region is 54.2 cm and the mean annual low and high temperatures are 3.9 and 35^{o} C, respectively. Installation of the VMS was completed in April of 2021. Sensors and sampling ports on the VMS were installed at 147, 246, 344, 442, 541 and 639 cm below the soil surface. During the VMS installation, soil samples were collected at the listed depths. Pipette texture analysis yielded the upper 3 m of the unsaturated zone to be a very fine clay and the bottom 4 m to be a clay to clay loam (Table 1). Clay soils tend to shrink and swell with varying water contents, which leads to cracks forming during the dry season (***figure 5***). The cracks have the potential to facilitate rapid flow of water and solutes deeper into the soil profile thereby modifying the hydrology of the soils (Bandyopadhyay, 2003).

Table 1. *Esparto Vadose Sampling Port (VSP) depth and corresponding soil texture.*

VSP port	Depth (cm)	%Sand	%Clay	%Silt	Classification
1	147	18.016	70.048	11.936	Clay
2	246	17.536	74.464	8.00	Clay
3	344	38.016	31.04	30.944	Clay Loam
4	442	40.32	29.216	30.464	Clay Loam

5	541	23.808	57.952	18.24	Clay
6	639	25.6	57.696	16.704	Clay

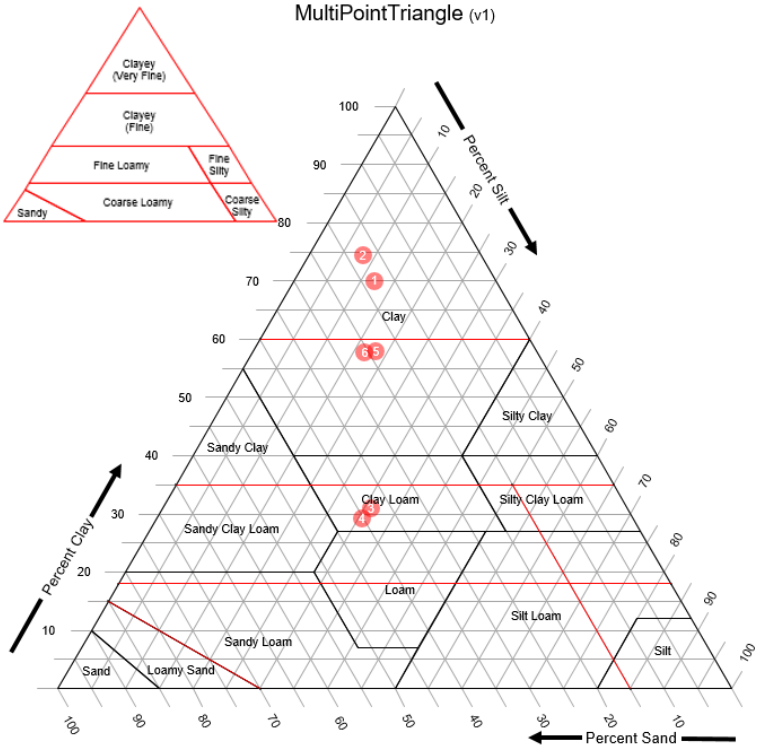

Figure 4. *Soil texture class based on percent sand, silt, and clay for every VSP port depth. Soil texture triangle provided by the U.S. Department of Agriculture.*

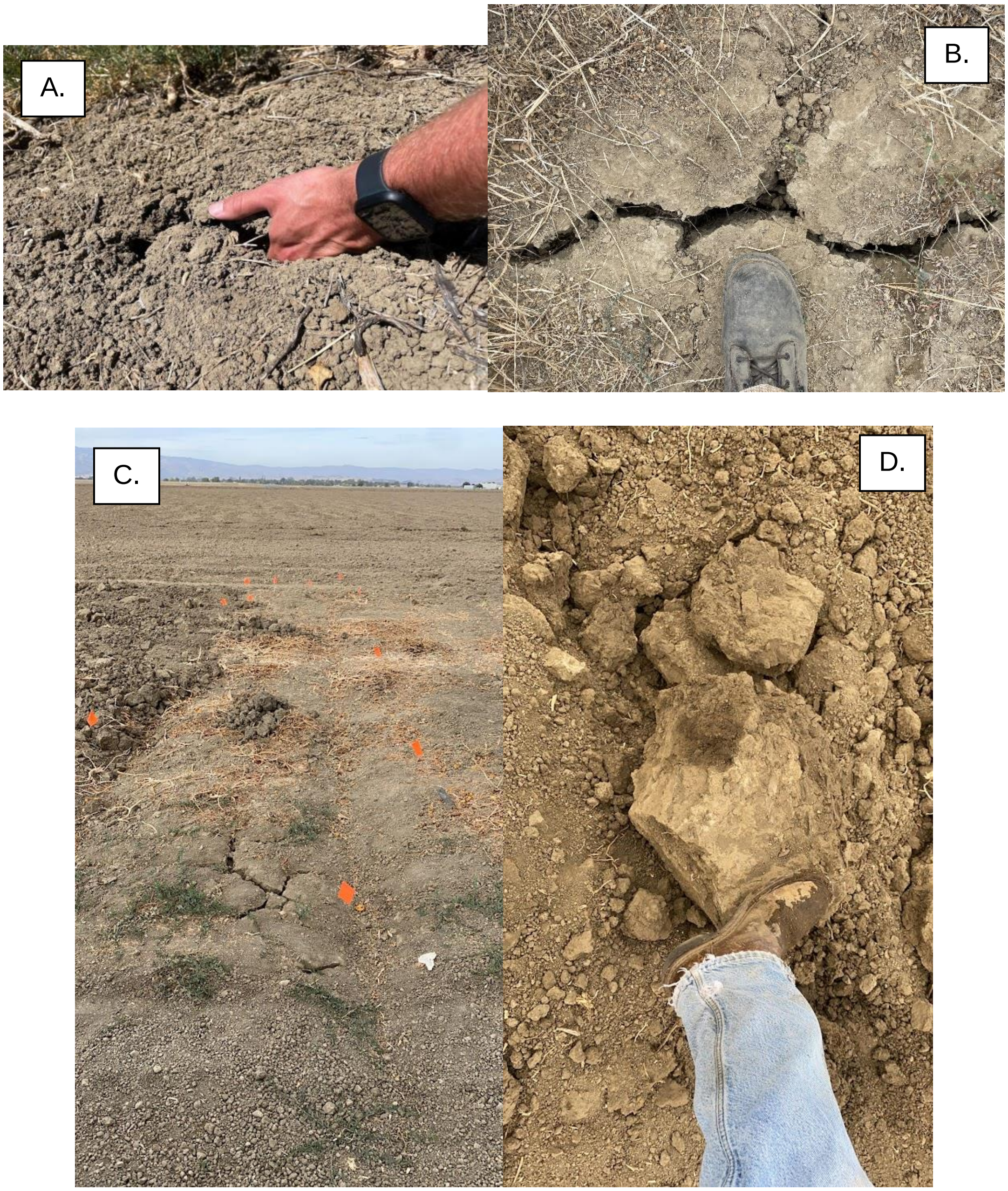

Figure 5. *Large cracks observed in the field with hand and boot for scale (A. and B.). Cracks above the VMS (C.) and Esparto soil aggregates formed by heavy clay (D.).*

After the Br^- tracer application, VMS pore water sampling was conducted on a weekly basis except after significant precipitation events (over 1 cm). The potassium bromide (KBr) tracer was applied on December 12th, 2021. Sampling continued throughout the winter and ended in April 2022 when bromide concentrations returned to pre-application values.

Site 2: Bowman Almond Orchard near Modesto California

The Bowman almond orchard is a 60 ha almond orchard west of Modesto, California. Walnut and almond orchards, vineyards, and dairy farms make up the majority of the surrounding landscapes. The grower uses surface drip systems to irrigate and fertigate the orchard. The site is located on a mix of Oakdale sandy loam (45.5%), Modesto clay loam (19.7%) and Dinuba fine sandy loam (28.8%) (USDA, 2023). The sand soils are well drained and have very low runoff and high saturated hydraulic conductivity. The clay loam series has a high runoff and moderately low saturated hydraulic conductivity. The semi-arid climate produces 33.3 cm precipitation annually and the region's low and high mean annual air temperatures are 4^{o} and 35.6^{o} C. The VMS was installed on August 9th, 2022. Sensors and sampling ports on the sleeve are at 40, 60, 240, 360, 480 and 620 cm below the soil surface. Soil samples were taken at these depths from the auger during installation. Texture analysis was performed using the pipette method, which showed a moderately homogenous sandy loam at the top two meters and a sandy clay loam through the bottom four meters (***Table 2***).

Table 2. *Bowman orchard near Modesto CA, Vadose Sampling Port (VSP) depths and corresponding soil textures.*

VSP	Depth (cm)	%Sand	%Clay	%Silt	Classification

1	40	72.224	3.584	24.192	Sandy Loam
2	60	66.912	4.032	29.056	Sandy Loam
3	240	81.856	3.84	14.304	Loamy Sand
4	360	83.008	4.064	12.928	Loamy Sand
5	480	85.024	2.56	12.416	Loamy Sand
6	620	82.976	3.616	13.408	Loamy Sand

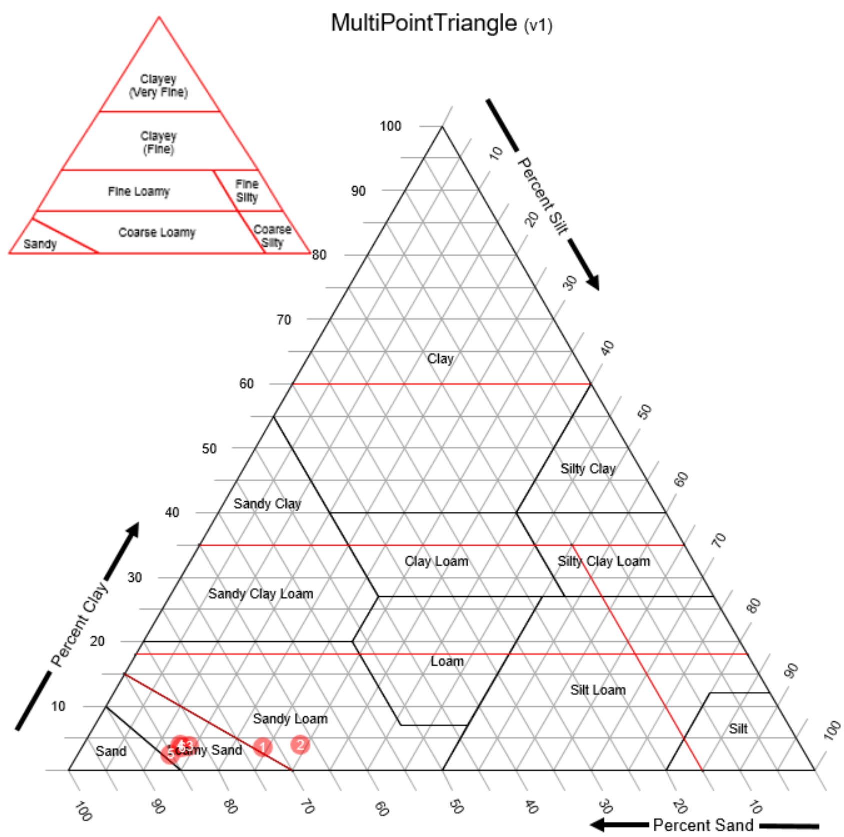

Figure 6. *Soil texture classes based on percent sand, silt, and clay for each VSP depth (.4-6.2m) for the Bowman Orchard near Modesto, CA. Textural triangle provided by the U.S. Department of Agriculture.*

VMS pore water sampling was conducted on a weekly basis except after significant precipitation events (over 1 cm). The potassium bromide (KBr) tracer was applied on January 12th, 2023. VMS pore water sampling continued through July 2023.

Site 3: Booth Ranch Citrus, near Orange Cove California

Orange Cove, California, is a small farming community 50 km southeast of Fresno, CA. Large scale citrus, cherry, and almond operations dominate the area. The study site is a 73 ha Valencia Orange orchard located 8 km to the West of the city of Orange Cove. The grower uses a micro-sprinkler irrigation and fertigation system. The soil unit that comprises this site is a San Joaquin loam consisting of moderately well-draining alluvial soils derived from granitic rock (USDA, 1999). The VMS was installed on August 8th, 2022 with VSP sampling ports on the sleeve at 40, 140, 260, 390, 550 and 750 cm below soil surface. Soil texture analysis showed the soil composition of the site ranges from sandy loam at the shallow depths (0-2 meters) to sandy clay loam in the deeper reaches of the vadose zone (5-7 meters).

Table 3. *Booth ranch near Orange Cove, CA Vadose Sampling Port (VSP) depths and corresponding soil textures.*

VSP	Depth (cm)	%Sand	%Clay	%Silt	Classification
1	40	66.336	14.912	18.752	Sandy Loam
2	140	61.248	13.824	24.928	Sandy Loam
3	260	53.984	25.376	20.64	Sandy Clay Loam
4	390	48.544	29.696	21.76	Sandy Clay Loam

5	550	51.808	21.216	26.976	Sandy Clay Loam
6	750	52.672	22.752	24.576	Sandy Clay Loam

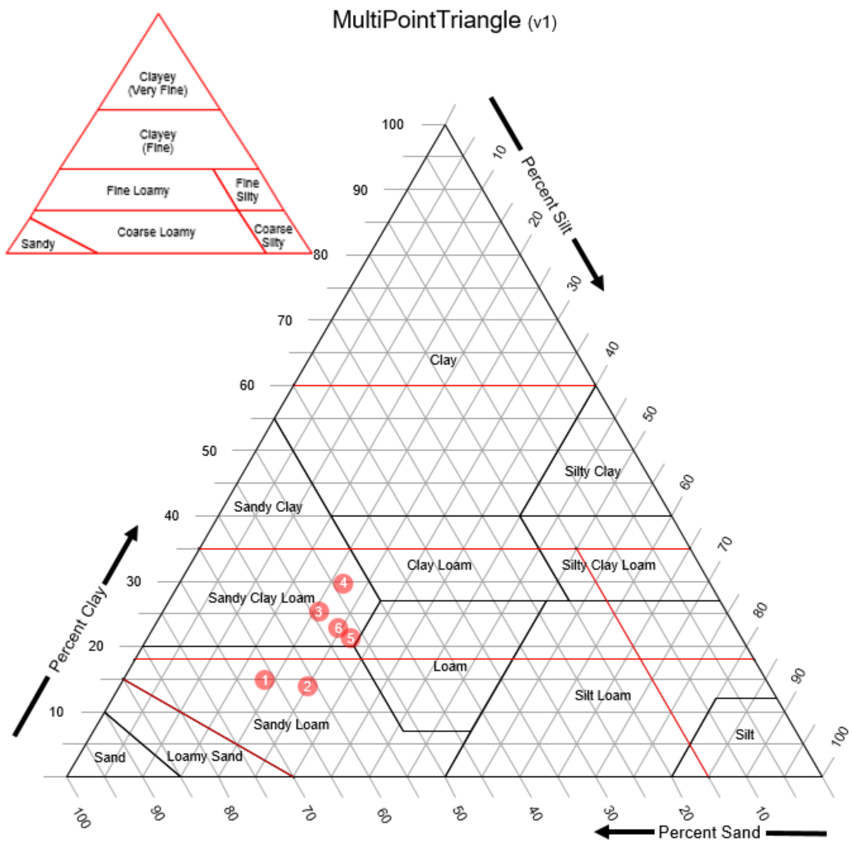

Figure 7. *Soil texture class based on percent sand, silt, and clay for each VSP depth (.4-7.5m) for Booth Ranch site near Orange Cove CA. Multipoint triangle provided by the U.S. Department of Agriculture.*

The climate is semi-arid with average precipitation at 31.3 cm annually. The mean annual high and low air temperatures at the site are 36.1° C and 4.4° C, respectively (US Climate Data, 2023). The KBr tracer was applied on May 19th, 2023.

2. HYDRUS 1D Model Inputs

A HYDRUS 1D model was developed for each sited to simulate solute transport of the KBr tracer with nonlinear cation adsorption prediction based on the findings of Lai and Jurinak (1971). A model with six soil material layers was created using textures generated from soil samples corresponding to the depths of each VSP for each site. The model was run at a daily time step except for the Booth site, which was run at an hourly time step due to the short duration of the study period. Model resolution followed 1 cm length unit for each layer. Time-variable boundary conditions was set for the model that followed field conditions (i.e. irrigation/precipitation and ET values). The hydraulic model selected was a single-porosity van Genuchten-Mualem with no hysteresis. Water flow parameters were selected using the Rosetta Lite v1.1 neural network prediction using percentages of sand, clay, and silt for each soil layer. Rosetta models hydraulic properties using pedotransfer functions with limited input data (USDA, 2023).

Table 4. *Esparto field site Soil Hydraulic Properties*

Layer	Q_r	Q_S	*Alpha*	*n*	K_S	*I*
1	0.1017	0.484	0.0189	1.136	15.93	0.5
2	0.101	0.4855	0.0202	1.1382	15.51	0.5
3	0.0782	0.4241	0.015	1.3819	5.45	0.5
4	0.0759	0.4184	0.0154	1.3866	5.89	0.5
5	0.095	0.4765	0.0173	1.2709	15.18	0.5

6	0.0956	0.472	0.0234	1.1978	15.15	0.5

Table 5. *Bowman orchard Soil Hydraulic Properties*

Layer	Q_r	Q_S	*Alpha*	*n*	K_S	*I*
1	0.0314	0.394	0.0427	1.486	73.58	0.5
2	0.0305	0.3956	0.0361	1.4277	65.97	0.5
3	0.0387	0.3873	0.0428	1.8137	121.27	0.5
4	0.0404	0.3859	0.0416	1.8815	134.38	0.5
5	0.0397	0.3875	0.0427	2.0776	177.72	0.5
6	0.0394	0.3869	0.0424	1.8899	136.37	0.5

Table 6. *Booth ranch Soil Hydraulic Properties*

Layer	Q_r	Q_S	*Alpha*	*n*	K_S	*I*
1	0.0509	0.3832	0.0304	1.383	30.82	0.5
2	0.0487	0.3864	0.0263	1.3895	28.66	0.5
3	0.0679	0.3945	0.0234	1.3364	11.64	0.5
4	0.0644	0.4	0.0172	1.4033	11.52	0.5

5	0.0628	0.396	0.0197	1.3853	13.54	0.5
6	0.0648	0.3957	0.0212	1.3669	12.82	0.5

Layer is soil layer corresponding to VSP depth; Q_r is the residual soil water content; Q_S is saturated soil water content; Alpha and n are parameters in the soil water retention function; K_S is the saturated hydraulic conductivity; I is the tortuosity parameters in the conductivity function.

An atmospheric boundary with surface layer was used as upper boundary in the model, while free drainage was set as lower boundary condition. Solute transport followed the Crank-Nicholson time weighting scheme with a Galerkin Finite Element space weighting scheme, both recommended in view of solution precision (Simunek, 2008). Initial water contents for each layer were specified in a graphical environment using the values measured by the TDT sensors.

Table 7. *Initial water content (W.C.) inputs for each layer in the HYDRUS models developed for the three sites.*

Layer	Esparto W.C. (%)	Bowman W.C. (%)	Booth W.C. (%)
1	43.2	28.8	28.6
2	29.5	35.7	38.17
3	33.5	18.5	42.9
4	35.4	6.9	37
5	37.3	8.5	40.9
6	34.3	22.6	30.9

Observation points were added at depths corresponding to each VSP to obtain outputs for pressure head, water contents, and concentration. Root water uptake was added to the Bowman and Booth models due to the presence of permanent crop vegetation during the experiment. Crop water uptake was simulated using the Feddes (1977) water stress response function with no solute uptake being that our study was primarily in the winter in Bowman and the speed of solute transport would likely exceed tree uptake at Booth .

3. *Tracer Application and Treatments:*

Bromide has been used in many subsurface hydrology transport studies and is considered to be a safe and conservative tracer (Levy & Chambers, 1987). Applying a volume of bromide solution above the VMS sleeve would infiltrate the soil and be collected by the pore water samplers at different depths. Application and concentration of bromide followed Weissman et al. (2020). To ensure that the tracer would be observed by the VMS, an irrigation application system was built using drip lines that would cover a pre-defined area above the sleeve. The drip system was constructed using a 5 cm PVC main line to which 14 drip lines were connected. The 2 cm diameter drip lines were spaced 30 cm apart and drippers within the lines were spaced every 30.5 cm (12 inches). The total width and length of the drip system was 4.2 m by 9.36 m. Dripper discharge was factory rated at 2.3 L/min but were measured to be 2.4 L/min. With a total of 434 drippers, the system put out 954 L/hour. A booster pump and pressure regulator were required to maintain the factory required water pressure for optimal dripper discharge. An 800-liter, vertical plastic tank was connected to the drip system using a series of irrigation hoses and fittings. A 500 ppm Br^- solution was prepared for each experiment by dissolving 274 grams of KBr (ACS reagent ≥99%) in 378.5 liters of irrigation water.

Figure 8. *Tracer application system*

Application of the bromide tracer was replicated at all three study sites. Precipitation and/or irrigation provided the water used to move the tracer through the soil profile. Precipitation and daily reference evapotranspiration (ET) values were downloaded from the nearest California Irrigation Management Information System (CIMIS) weather station. Reference ET values were converted to actual ET by multiplying the monthly crop coefficient from Sanden (2007) with the potential ET estimated by the closes CIMIS station. During the monitoring period, the Esparto and Bowman sites received 157.4 mm and 153.9 mm of rainfall, respectively. Data provided by the grower at the Bowman site yielded 259 mm of irrigation applied over the study period. The final tracer application at the Booth site was completed during the late spring therefore precipitation was negligible. 110 mm of active irrigation was used to push the bromide through the sandy soils of the Booth site. Irrigation events consisted of 23 minutes in which 10mm of water was applied. Irrigation occurred every 4 hours to assure that the tracer would be flushed through the entirety of the vadose zone. With each irrigation event, samples were collected from the VMS and vacuum was applied for four hours to collect a new sample. Sample volume varied from 2ml to 15ml across all VSPs.

Table 8. *Site based treatment, study period, and facilitated flow.*

Site	*Tracer (Concentration/Amount)*	*Study Period*	*Facilitated flow*
Esparto	*KBr 500ppm/378 liters*	*December 7th 2021-March 30th 2022*	*Precipitation: 157.4mm*
Bowman Orchard	*KBr 500ppm/378 liters*	*January 12th 2023-July 5th 2023*	*Precipitation/Irrigation: 408mm*
Booth Ranch	*KBr 500ppm/378 liters*	*May 19th 2023-May 22nd 2023*	*Irrigation: 110mm*

4. Bromide Analysis: Ion Selective Electrode

Bromide concentrations were measured using a Thermo Scientific™ Bromide ionplus® Sure-Flow® Solid State Combination Ion Selective Electrode. The ion selective electrode (ISE) is a potentiometric sensor that uses a selective membrane that responds to a specific ion concentration in a solution. The electroanalytical sensor maintains a degree of selectivity to a unique ion species (K. Štulík, 2005). When submerged in a solution containing bromide ions, an electrical potential is created across the sensing element and is measured against the reference potential. The bromide ion concentration that corresponds with the measured potential can be described through the Nernst equation (Thermo Scientific, 2008).

Equation 4. *Nernst Equation.*

$$E = E_0 + S\, log(A)$$

Where E is the measured electrode potential, E_0 is the reference potential (a constant); A is the level of bromide ion in solution; S = electrode slope (around -57mV per decade), where $S = 2.3\ \frac{RT}{nF}$: R & F are constants, T is temperature (degrees K), and n = ionic change.

The specific model of ISE used in this study uses a combination electrode and has the sensing as well as reference cells built into one electrode, allowing for reduction in the required amount of sample. The detection limit of the electrode is less than .4ppm Br^-. Lower concentrations detection is limited by the electrode's response to ions within the sample and dissolved ions from the sensing element (Thermo Scientific, 2008). Electrode potentials are also influenced by changes in the sample temperature. The absolute potential of the reference electrode is subject to change with temperature fluctuation because of the solubility equilibria. Samples and standard solutions during analysis were within 1 ^{o}C of each other.

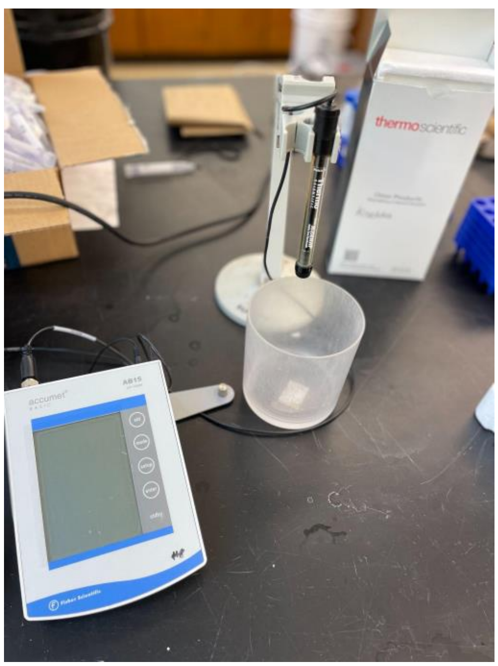

Figure 9. *Thermo Scientific™ Bromide ionplus® Sure-Flow® Solid State Combination Ion Selective Electrode.*

5. Change in Storage Computation

The bromide mass balance was estimated by using the volumetric water content and bromide concentrations at different depths and time steps. Prior to tracer application, soil pore concentrations were measured together with the volumetric water content at all sampling ports. By multiplying the pore water concentration (mg/L) with the water content (unitless), the initial soil bromide was estimated. Subtracting the initial bromide from the final day's concentration gives the change of storage at each VSP layer.

Equation 5. *Change in soil bromide storage.*

$$C_i + \Delta S = C_f$$

C_i is initial concentration; ΔS is change in storage; C_f is final concentration.

Results

1. Site 1: Esparto

Initial water content varied throughout the soil profile with the upper most water content sensor reading 43.22% and the deepest reading 34.55%. The TDT sensor at 2.46 m read the least water content at 29.51%. Volumetric soil water content increased dramatically through all sensor depths following a significant rainfall event (6.27cm/day) on December 13th, 2023. As the soil became saturated, water contents rose to near 50% at sensor 4 and 5 located at 4.42 and 5.41 m respectively. The soil retained high levels of saturation for 6 days before the profile began to drain to field capacity, where it remained for a majority of the sampling period. Soil temperature decreased substantially at the upper two sampling depths following the rain events, whereas the rest of the profile experienced a slow gradual decrease. An increase in temperature of the shallowest sensor was captured towards the end of the study.

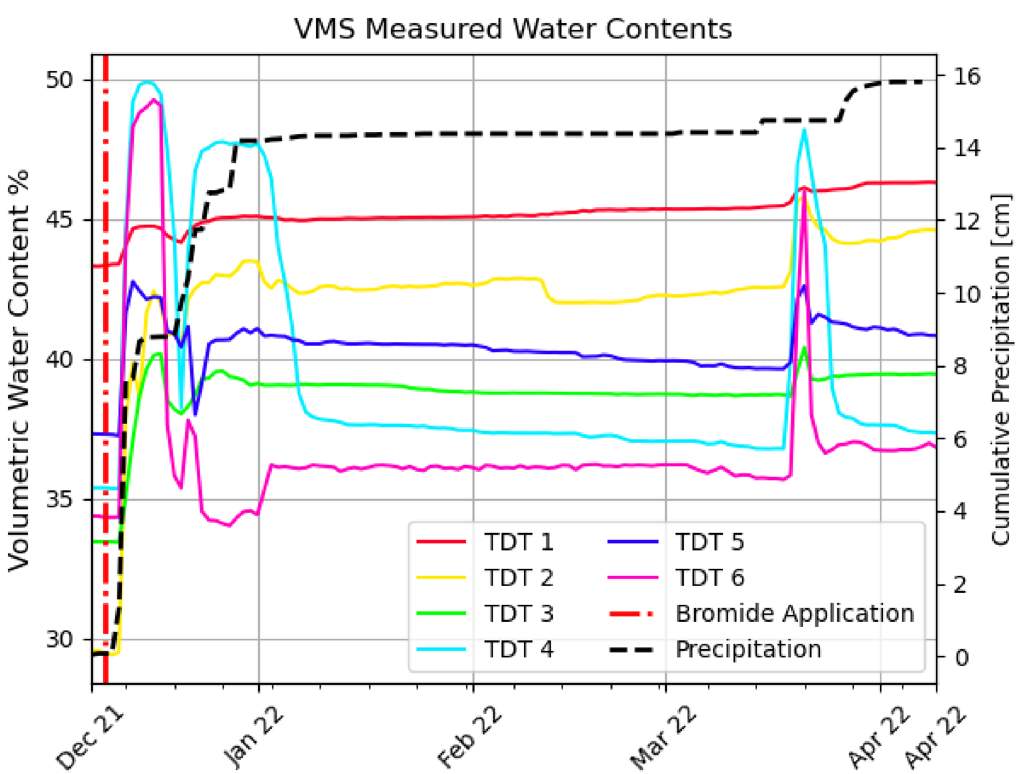

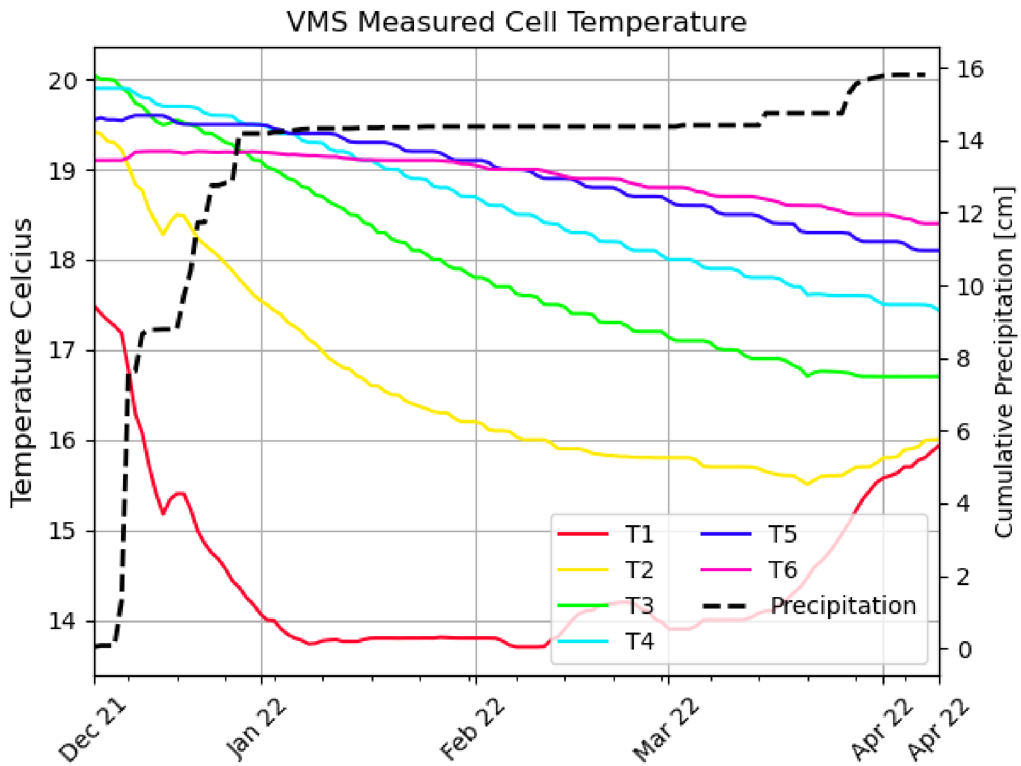

Figure 10. *Esparto measured soil volumetric water content (upper) and measured temperature (lower) at different VSPs in the VMS sleeve, with cumulative precipitation (cm) and the bromide application date.*

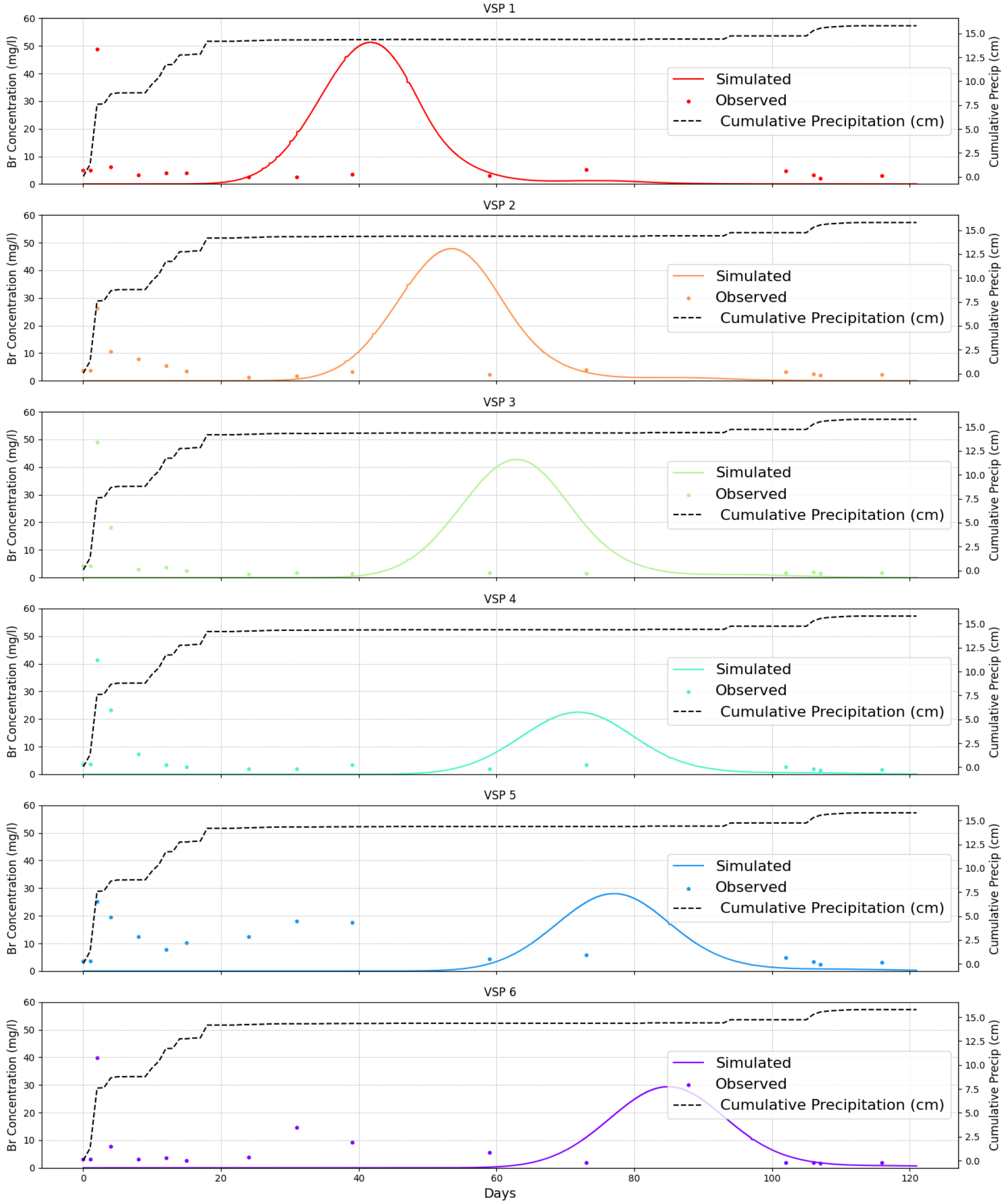
VSP 1
VSP 2
VSP 3
VSP 4
VSP 5
VSP 6
Simulated
Observed
Cumulative Precipitation (cm)
Br Concentration (mg/l)
Cumulative Precip (cm)
Days

Figure 11. *Bromide concentrations (mg/l) observed at six depths in the VMS sleeve in Esparto, CA and simulated with HYDRUS 1D between December 2021 and April 2022. Note that plot VSP1 also shows cumulative precipitation (cm) and the bromide application date.*

Profile average Br^- concentrations observed before tracer application were consistently at around 3.88 mg/L. The highest concentration was measured in the shallow sampler at 4.95 mg/L Br^-. Similar to the water content, the Br^- concentration increased at a rapid rate across all sampling ports following the tracer application and subsequent precipitation. The highest concentrations were measured at samplers 1 and 3 at 49 mg/l Br^-. Concentrations returned to pre-application levels approximately 10 days after the breakthrough peak. A secondary peak was detected in samplers 5 and 6, 30 days after the initial application, reaching 18 and 14 mg/L Br^-, respectively. The HYDRUS 1D simulated concentrations of the bromide tracer are as expected under ideal conditions and given the soil hydraulic properties and breakthroughs at all depths later than those observed. The breakthrough at VSP 1 was simulated to be within 65 days with a peak of 51.3 mg/l Br^- at day 40. The simulation for VSP 2 resulted in a peak of 47.8 mg/l Br^- and complete breakthrough after 80 days. VSPs 3, 4, 5, and 6 were simulated to have peaks concentrations of 47.5, 42.5, 22.8, 28.0 and 29.3 mg/l Br^- and complete breakthroughs after 90, 95, 105 and 110 days, respectively. Observed peaks for VSPs 4, 5, and 6 were 41.4, 25.2 and 39.7 mg Br^-, respectively. Change in soil storage of bromide decreased at all depths, demonstrating that the bromide tracer was completely leached from the entire soil profile (***Table 8.)***.

Table 9. *Change in Esparto soil bromide concentration from the start to the end of the study period at each VSP.*

Soil Br^- Concentration	VSP 1	VSP 2	VSP 3	VSP 4	VSP 5	VSP 6
Initial	2.14	1.13	1.39	1.29	1.35	1.05
Final	1.36	1.04	0.657	0.685	1.26	0.681
Change in storage	-0.786	-0.087	-0.735	-0.605	-0.093	-0.368

2. Site 2: Bowman

Initial water contents within the soil profile at the Bowman orchard varied greatly. Sensors 1 and 2 recorded values of 32% and 59% which were likely a result of the 3.4 cm precipitation that occurred on January 10th, 2023 (two days prior to the application of the tracer). Water contents for the bottom sensors were around 7% for sensors 4 and 5. TDT sensor 6 at 6.2 m read a soil water content of 22.2% on January 12th. Data from a monitoring well within 10 meters the sleeve indicated that TDT sensor 6 was likely influenced by the capillary fringe of the groundwater table. Water contents at the upper three sensors decreased over the next months, demonstrating that the soils were draining. Following said draining, sensors 4, 5 and 6 increased to ~15%, 12% and 35% respectively, indicating water was moving from the layers above. The two shallow sensors fluctuated with precipitation and irrigation later in the sampling period. Drainage occurred following the last significant precipitation event on March 28th and sensors 1 and 2 reached lows of ~15% until irrigation began on March 20th in which the sensors would increase to an average of ~25% and 22% through the rest of the study period. The water content would fluctuate with each irrigation and subsequent drainage/root uptake. Temperature sensors 1, 2 and 3 gradually increased starting in March of 2023, likely as a result from the increasing ambient air temperature from ~13º C to ~19º C. Temperature sensors in the bottom layers would decrease slightly before increasing to around 17º C.

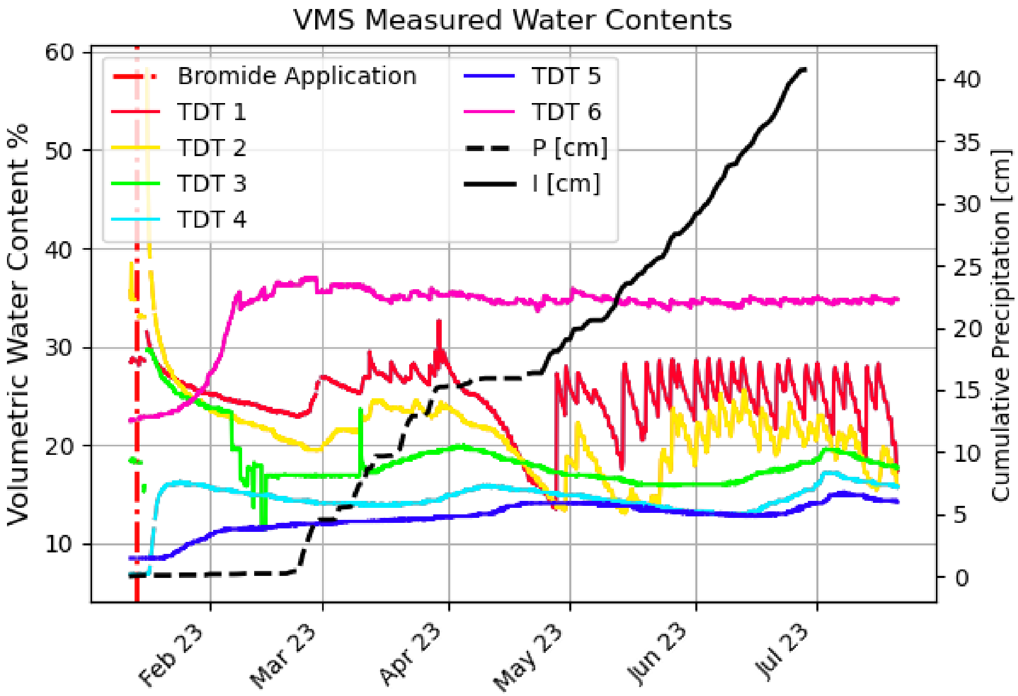

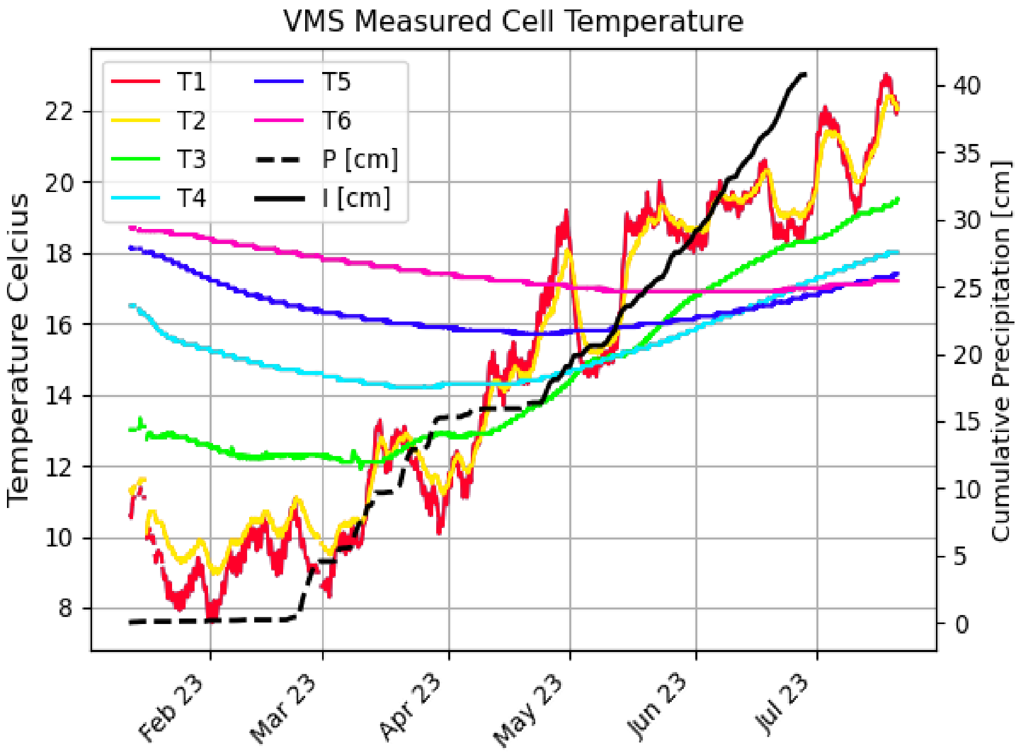

Figure 12. *Volumetric water content (upper) and soil temperature (lower) measured at different sensor depths in the VMS sleeve installed at the Bowman orchard from January 10th, 2023 to July 20th, 2023. Note, cumulative precipitation (cm), irrigation (cm), shown in black dashed and solid line respectively. Bromide application shown by dashed red line on January 12th, 2023.*

Bromide concentrations in the soil pore water prior to the Br^- tracer application was measured close to 1.5 mg/l Br^- for every sampler at the Bowman orchard. 15 days after application of the tracer, the concentration observed at VSP 1 reached a peak of 17.1mg/L Br^-. Concentrations would remain around 12 mg/l Br^- before returning to background levels 70 days after application. Following the decrease in concentration in VSP 1, VSP 2 observed an increase until reaching the peak of 12.45 mg/l Br^- approximately 150 days after initial tracer application. VSP 2 concentration would return to initial levels around 190 days into the study. Observed peak concentrations for VSP 3 and 4 were 4.93 and 6.4 mg/l Br^- at day 175 and 189, respectively, and would never return to background concentrations. Similar to the Esparto simulations, the Br^- concentrations from the HYDRUS model results were as expected. VSPs 1, 2, 3, 4, 5, 6, had a simulated peak concentration of 14, 7.4, 4.9, 2.4, 2.8, and 2.9 mg/l Br^- with complete breakthroughs after 82, 110, 122, 130, 139, and 147 days, respectively. The change in bromide storage within the soil profile would indicate that the tracer had been completely leached out of the top layer. Increases of soil water bromide from application till final day of study indicate the tracer is yet to leach out of the bottom 5 layers of the soil profile.

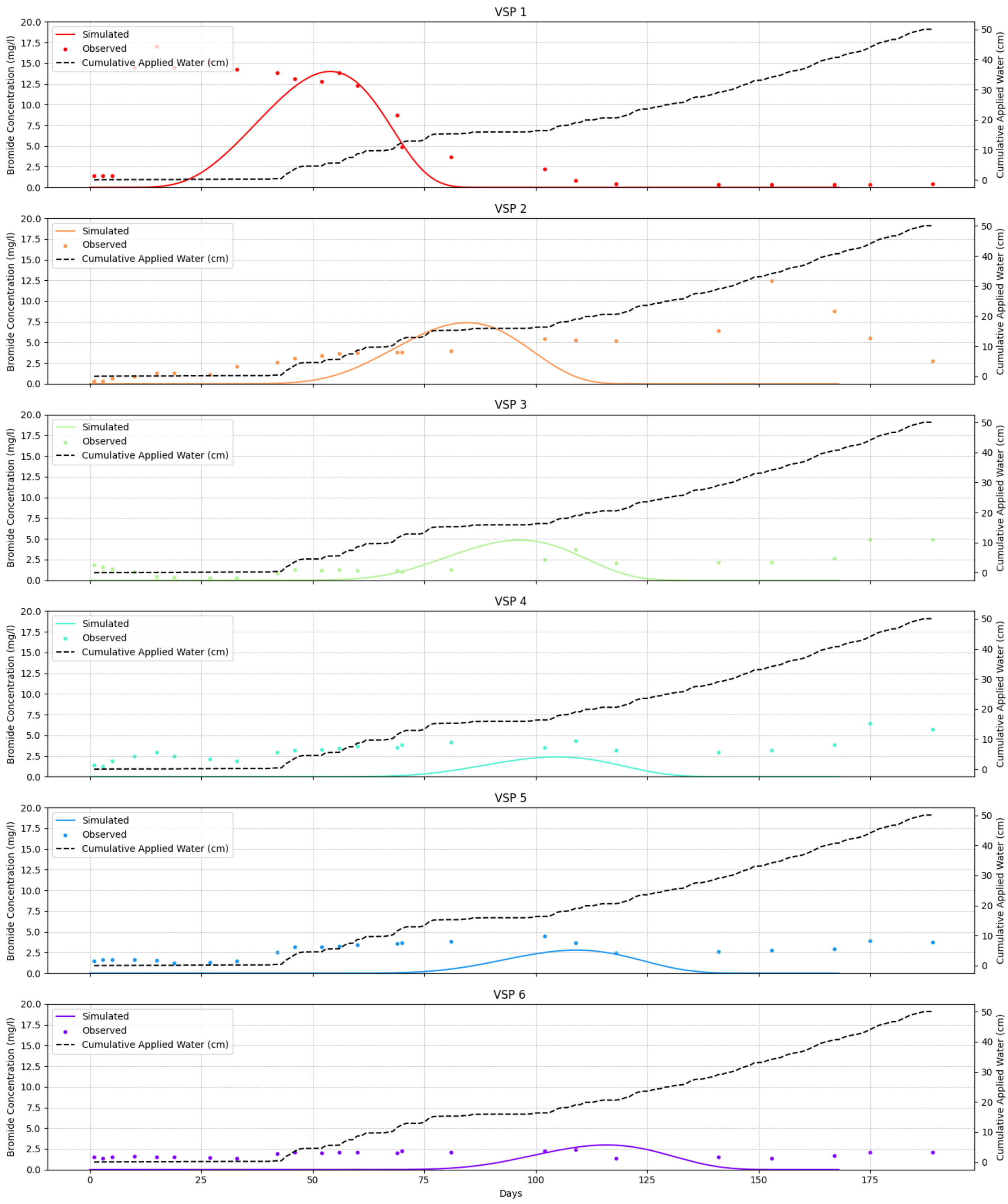
VSP 1
VSP 2
VSP 3
VSP 4
VSP 5
VSP 6
Simulated
Observed
Cumulative Applied Water (cm)
Bromide Concentration (mg/l)
Cumulative Applied Water (cm)
Days

Figure 13. *Bromide concentrations (mg/l) observed at the Bowman orchard and simulated with HYDRUS 1D plotted by day starting January 10th, 2023 to July 20th, 2023. Note that plots also show the cumulative applied water (cm) on secondary y axis.*

Table 10. *Change in Bowman soil bromide storage from the start to the end of the study period at each VSP.*

Soil Br^- Concentration	VSP 1	VSP 2	VSP 3	VSP 4	VSP 5	VSP 6
Start	0.403676	0.123887	0.334634	0.099018	0.126742	0.335598
End	0.079688	0.464954	0.8651	0.92128	0.538345	0.726735
change in storage	-0.32399	0.341067	0.530466	0.822262	0.411603	0.391137

3. Site 3: Booth Ranch

Water content recorded by the TDT sensors along the sleeve would indicate the soil was quite saturated prior to tracer application. Sensor 1 and sensor 6 would remain stable at ~30% for a majority of the study period. Sensor 3 measured the highest W.C. at 43% and would continue to stay at 40% while sensors 2 and 4 would stay at 37% and 38% for the duration of the study. The temperature readings indicate little change in the soil profile. Sensors 1 and 2 would increase ever slightly to 18.8^{o} C and 16^{o} C. Sensors 3, 4, 5 and 6 would remain around 14.3^{o} , 14.6^{o}, 15.7^{o} and 16.8^{o} C, respectively.

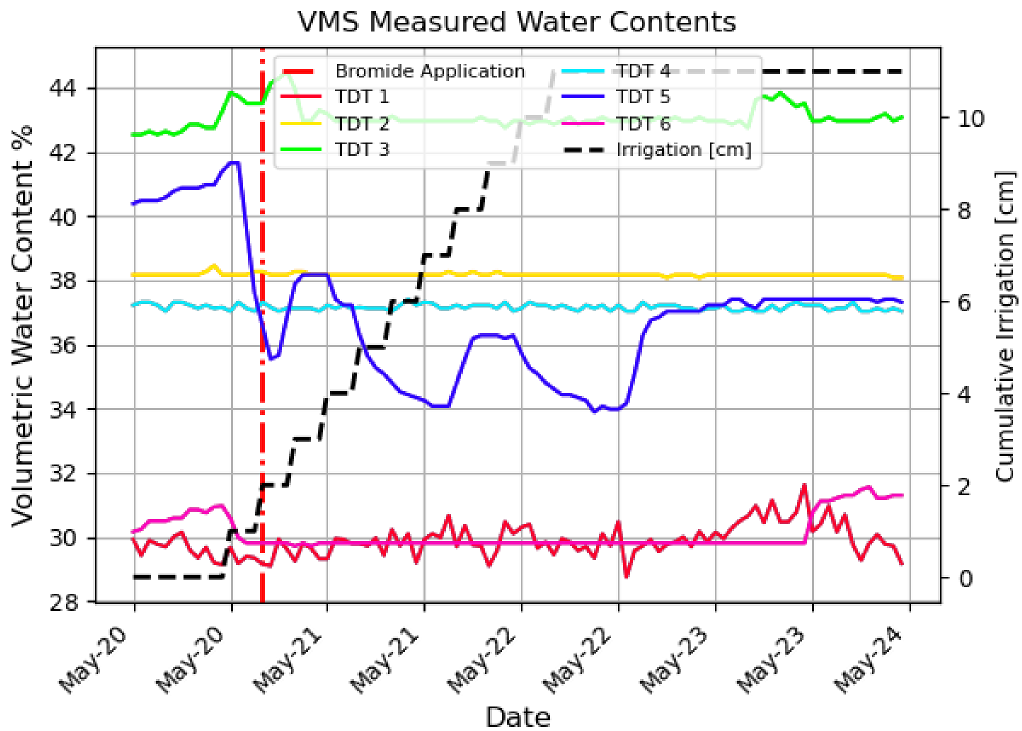
VMS Measured Water Contents
Bromide Application
TDT 1
TDT 2
TDT 3
TDT 4
TDT 5
TDT 6
Irrigation [cm]
Volumetric Water Content %
Cumulative Irrigation [cm]
Date
May-20
May-20
May-21
May-21
May-22
May-22
May-23
May-23
May-24

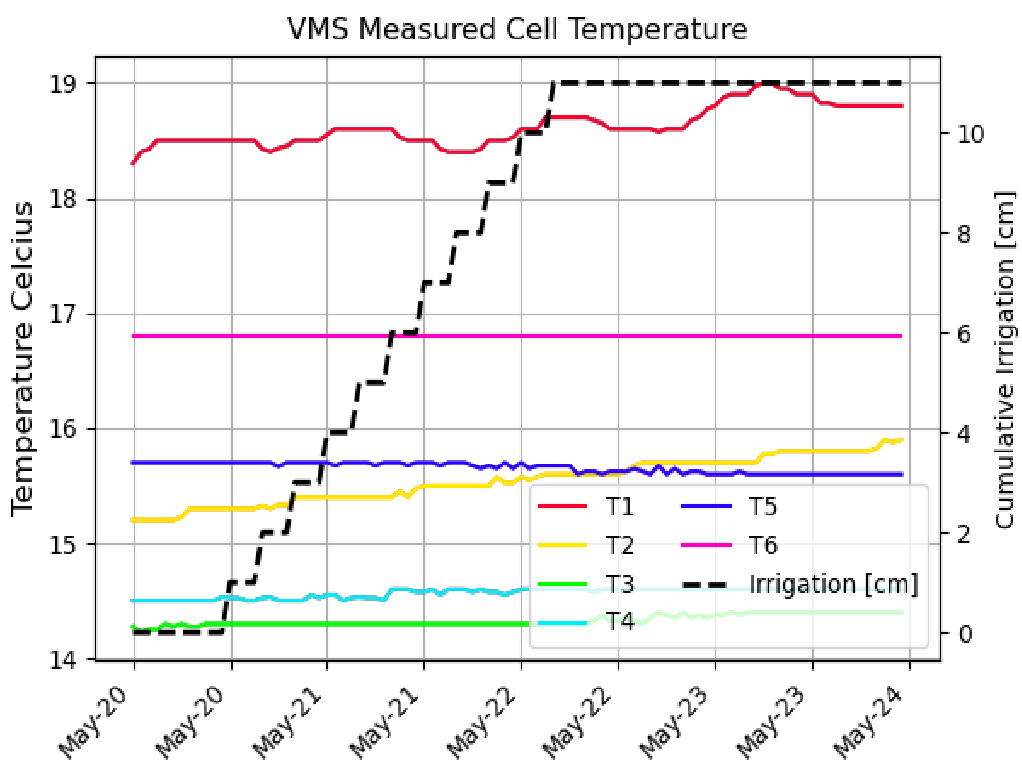
VMS Measured Cell Temperature
T1
T2
T3
T4
T5
T6
Irrigation [cm]
Temperature Celcius
Cumulative Irrigation [cm]
May-20
May-20
May-21
May-21
May-22
May-22
May-23
May-23
May-24

Figure 14. *Booth measured volumetric water content (upper) and temperature (lower) at different VSP's in the VMS sleeve, with cumulative irrigation (cm) and the bromide application date from May 20th to May 23rd 2023.*

Initial bromide concentrations from pore water solution were relatively high at 6.93 mg/L Br^- in VSP 1 and 11.3 mg/L Br^- in VSP 2. VSP's ports 3,4,5, and 6 observed values close to 9.5mg/L Br^- prior to tracer application. Concentrations increased slightly (~2 mg/L) in VSP 1, 2, and 3 four hours after tracer treatment at 12:00pm on May 20^{th} , but returned to pre-application levels following another four hours. VSP 5 and 6 experienced a decrease in bromide concentrations over the course of the study. HYDRUS simulated Br^- concentrations resulted in a complete breakthrough in VSP 1 in 1.2 days with a peak of 29.4 mg/l Br^- at .7 days. VSP 2 had a simulated concentration of 6.9 mg/l Br on the last day of simulation. Simulated breakthroughs for VSPs 2, 3, 4, 5, 6 were non-existent with minimal increases in bromide detected in the lower 4 VSPs. The change in soil tracer storage indicates that the Br^- tracer resides in the upper three meters and is yet to flow into the 4^{th}-6^{th} meter of the profile shown by VSP 4,5,6 (***Table 10***).

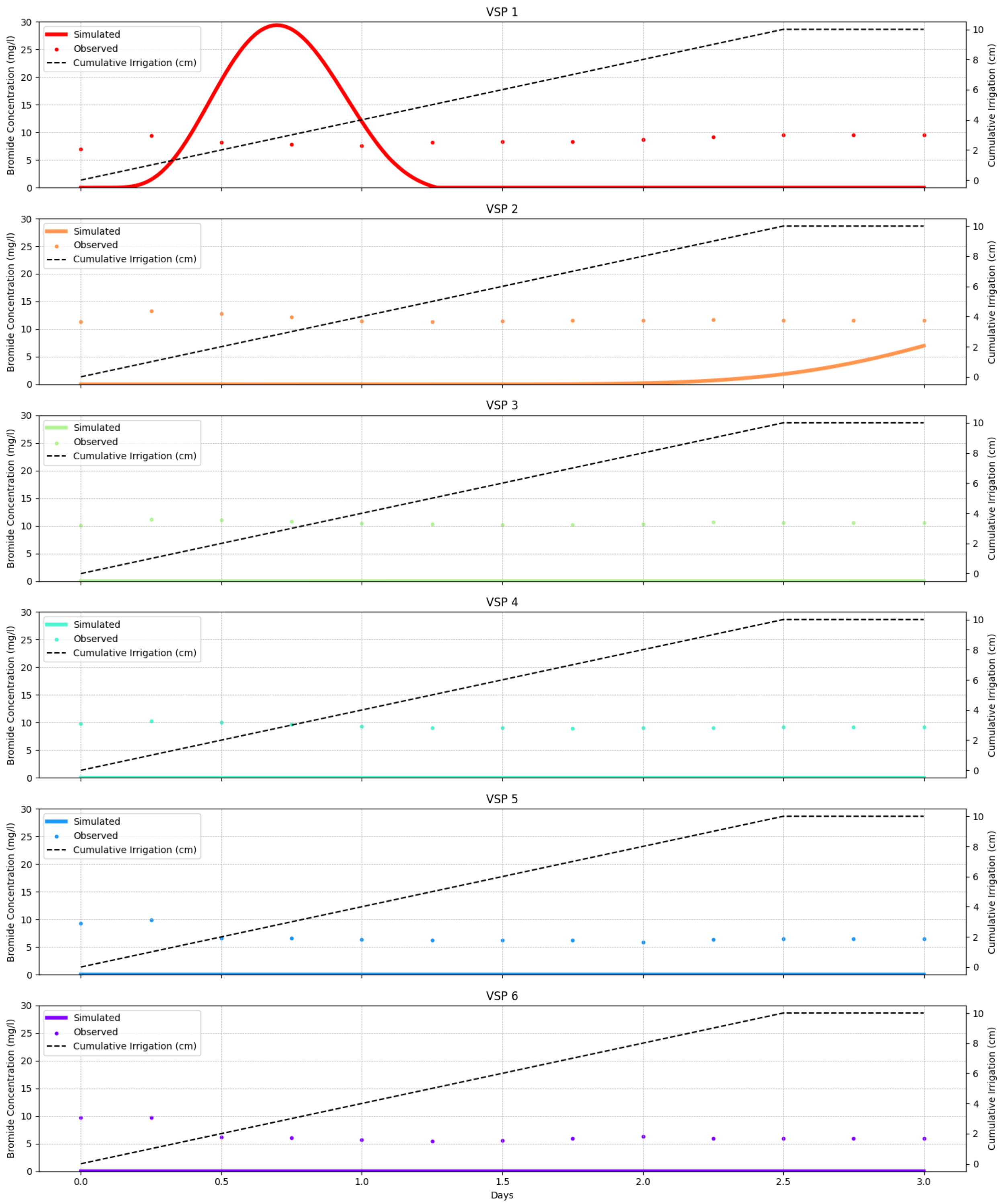
VSP 1
VSP 2
VSP 3
VSP 4
VSP 5
VSP 6
Simulated
Observed
Cumulative Irrigation (cm)
Bromide Concentration (mg/l)
Cumulative Irrigation (cm)
Days
0.0
0.5
1.0
1.5
2.0
2.5
3.0
0
5
10
15
20
25
30
0
2
4
6
8
10

Figure 15. *Bromide concentrations (mg/l) observed in Booth, CA and simulated with HYDRUS 1D plotted by day starting May 20th-24th, 2023. Note, that plots also show the cumulative irrigation (cm).*

Table 11. *Change in Bowman soil bromide storage from the start to the end of the study period at each VSP.*

Soil Br^- Concentration	VSP 1	VSP 2	VSP 3	VSP 4	VSP 5	VSP 6
Start	2.030	4.332	4.271	3.644	3.704	2.938
End	2.768	4.412	4.563	3.451	2.221	1.778
Change in Storage	0.737	0.081	0.292	-0.193	-1.484	-1.160

Discussion

The results of the experiment demonstrate the ability of the VPS vadose monitoring system to detect an applied tracer in three different soil systems. Bromide transport and water flow varied greatly across the three sites, which was expected due to the different soil textures and amounts of water applied at each site. Soil properties and water contents govern the percolation of water and the transport of the solute. The magnitude of the breakthrough peaks decreased with depth similar to other single-event tracer experiments (Weissman et al. 2020). The one-time application created plumes that dispersed vertically with infiltration through the deeper layers.

At the Esparto site a complete breakthrough of the Br^- tracer was observed at all VSP's within a day of the extreme precipitation event mentioned in the results. Preferential flow paths, either in the form of cracks in the soil were likely the explanation of this bromide signature. Unstable wetting fronts create 'finger flow' where flow and solute transport experience velocities much higher than those calculated under stable wetting fronts (Hendrickx and Flury, 2001). The high infiltration event led to an almost instantaneous increase in water contents in the profile as shown by the TDT sensors. The fast-moving wetting front is evidence that water flow exceeded the saturated hydraulic conductivity values expected of heavy clay soils (.5-1 cm/day). This was also indicated by the difference in simulated and observed tracer breakthroughs. The simulated solute transport followed soil water flow governed by these parameters resulting in a breakthrough in the deepest VSP at 29.4 mg/l at day 85, contrary to the breakthrough of 40mg/l observed in VSP 6 in only the 3^{rd} day after application. The secondary pulse of bromide observed in the deepest two sampling ports on day 31 after the Br^- tracer was applied demonstrates the slow drainage of residual bromide from the layers above, which had a saturated hydraulic conductivity that was 33% lower than the deeper vadose zone. The saturated hydraulic conductivity predicted by Rosetta and used in the HYDUS model was as low as 5.45 and 5.89 cm/day for layers 3 and 4. There was little correlation between the timing of the simulated breakthroughs, however, some of the peak VSP concentrations observed were in agreement to the modeled values. The highest concentration observed in VSP 1 was 48.9 mg/l Br^-, while the simulated peak was 51.3 mg/l. Observed and simulated peak concentrations in VSP 3 were 47.8 and 42.7 mg/l Br^- respectively. Finally, VSP 5 observed a peak of 25.2 mg/l Br^- and was simulated at 28 mg/l. Real-time monitoring of the soil water content and observed tracer concentrations demonstrated a dynamic percolation and non-steady wetting fronts, both expected in a heterogeneous soil profile.

The Bowman site received very little precipitation early on in the study. Solute transport to VSP 1 was facilitated by the residual soil water from a previous storm that had occurred 4 days prior to application and its subsequent drainage. The observed peak concentration for VSP 1 occurred earlier than the simulated peak, likely a result of the super saturated conditions upon application, however the complete breakthrough were similar in timing. Following the first rainfall event of 1.6cm/day, 45 days after initial application, the concentration would start to decrease in VSP 1 and increase in VSP 2 demonstrating that the tracer was gradually moving through the profile. Even with the added irrigation, water and solute movement was slow in the lower layers. The slight increases in water content at TDT 3 indicates that the grower is very efficient in irrigation and that little water was draining out of the root zone above. Vertical percolation via gravitational forces is limited in a soil undergoing desaturation. As the large pores empty, hydraulic conductivity decreases considerably. Water and solute would eventually reach the lower VSPs of 3, 4 and 5, illustrating an increase in observed concentration and water content towards the end of the study period. Knowing that VSP 6 was close to the groundwater table at the time of the experiment, changes in concentration were negligible due to the dilution of tracer from existing soil water. Similar to the Esparto model, the simulated values at the Bowman site were generally similar to the observed concentrations, however simulate and observed breakthrough curves had contrasting durations and peak concentrations. Simulated breakthroughs appeared earlier than observed, likely a result of the model inaccuracies in root water uptake for the trees.

The soil profile at Booth Ranch was close to saturation upon the tracer application as evident by the high, stagnant water contents across the profile with exception of TDT 5 which showed drainage for 1.5 days before returning to a steady state saturation. The amount of water in the soil pore space was large, which caused the concentrated bromide solution to be significantly diluted upon treatment. Background Br^- concentrations were higher than the other sites with an average close to 8 mg/l. The subsequent irrigation events would further dilute the solution, thus explaining the small change from background concentrations. A combination of the low Br^- concentration at the start of the experiment and saturated conditions created very low detection of the tracer across the VSPs. This low concentration could explain the reduction in observed concentration due to dilution effects (e.g. VSP 5 and 6). HYDRUS simulations indicated a complete breakthrough in VSP 1 and an increase in Br^- concentration in VSP 2, while VSPs 3-6 concentrations stayed relatively the same throughout the duration of the study with no change.

Chapter 3: Conclusions and Future Work

A Br^- tracer was applied to assess the performance of three distinct vadose monitoring systems (VMS) in detecting a constituent as it is transported through the unsaturated zone. The results of this study validate that the VMS is capable of monitoring transport of potential contaminants. Observed values were not as expected due to the initial storm severity, initial soil conditions and concentrations or their combination. The distribution of tracer concentrations was a result of flow mechanisms influenced by infiltration and soil properties as demonstrated in previous VMS studies (Fernandez et al., 2017). Cracks, wormholes, and the hydraulic properties of heterogeneous soils can create preferential flows which are difficult to identify as well as to quantify in their effect on flow and solute transport. The results of this study demonstrate that vadose zone infiltration is rarely uniform and subsurface monitoring is difficult due to the complexity of the soil matrix.

The study also provided valuable lessons for future experimental designs with the VMS. Observed values from each tracer experiment were influenced by the initial conditions of the soil profile including water content. Future tracer studies will use the application system to apply irrigation periodically to ensure equal water dispersion over the applied tracer. To facilitate the interpretation with computer models or analytical tools, the soil profile will be saturated prior to tracer application to ensure uniform flow. Using precipitation to facilitate solute transport is undesirable because it cannot be controlled and may lead to surface runoff if infiltration is low. Soil conditions should be suitable with no visible cracks, fissures, or other potential sources of preferential flow. Tracer application will take place when root uptake and evapotranspiration is negligible (i.e. when trees are dormant and field crops have been terminated).

In future tracer studies, the initial concentration of bromide will be increased to ensure detection at depth. Large amounts of applied irrigation will dilute the tracer with each infiltration event, therefor the concentration of bromide will be significant to overcome the dilution factor.

Finally, the use of electrical resistivity tomography (ERT) will be implemented in future VMS studies. Because subsurface electrical properties are indicative of soil water content and solute concentration, the ERT is a suitable tool to monitor flow characterization (Slater et al., 2000). Results from the ET would provide evidence of lateral tracer accumulation from layering of the soil profile.

References

Aharoni, Imri, Siebner H., Dahan, Ofer. Application of vadose-zone monitoring system for real-time characterization of leachate percolation in and under a municipal landfill. Waste Management. Volume 67. 2017. Pages 203-213, ISSN 0956-053X. https://doi.org/10.1016/j.wasman.2017.05.012.

Almarsi, Mohammad. Nitrate contamination of groundwater: A conceptual management framework. Environmental Impact Assessment Review, 2007.

Amiri, et al. Methods for Sample Collection, Storage, and Analysis of Freshwater Phosphorus. Water 2019.

Bandyopadhyay, K. K., Mohanty, M., Painuli, D. K., Misra, A. K., Hati, K. M., Mandal, K. G., ... & Acharya, C. L. (2003). Influence of tillage practices and nutrient management on crack parameters in a Vertisol of central India. Soil and Tillage Research, 71(2), 133-142.Anderson, M. P. (2005). Heat as a ground water tracer. Groundwater, 43(6), 951-968.

Barcelona, et al. A Guide to the Selection of Materials for Monitoring Well Construction and Groundwater Sampling. Environmental Science, 1983.

Bech, T. B., Rosenbom, A. E., Sørensen, S. R., & Jacobsen, C. S. (2017). Conservative tracer bromide inhibits pesticide mineralisation in soil. Environmental Pollution, 222, 404-411.

Brandi-Dohrn, F.M., Hess, M., Selker, J.S. and Dick, R.P. (1996), Field Evaluation of Passive Capillary Samplers. Soil Science Society of America Journal, 60: 1705-1713. https://doi.org/10.2136/sssaj1996.03615995006000060014x

California Department of Food and Agriculture. Fertilizer Research and Education Program. 2023.

California Water Boards, 2023. Irrigated Lands Regulatory Program. California Environmental Protection Agency.

Clutter, M. and Ferré, T.P.A. (2018), Examining the Potentials and Limitations of Using Temperature Tracing to Infer Water Flux through Unsaturated Soils. Vadose Zone Journal, 17: 1-8 170181. https://doi.org/10.2136/vzj2017.10.0181

Davis, S.N., Thompson, G.M., Bentley, H.W. and Stiles, G. (1980), Ground-Water Tracers — A Short Review. Groundwater, 18: 14-23. https://doi.org/10.1111/j.1745-6584.1980.tb03366.x

Dahan, O., McDonald, E.V. and Young, M.H., 2003. Flexible time domain reflectometry probe for deep vadose zone monitoring. Vadose Zone Journal, 2(2), pp.270-275.

Dahan, O., Talby, R., Yechieli, Y., Adar, E., Lazarovitch, N. and Enzel, Y. (2009), In Situ Monitoring of Water Percolation and Solute Transport Using a Vadose Zone Monitoring System. Vadose Zone Journal, 8: 916-925. https://doi.org/10.2136/vzj2008.0134

Delgado, J.A. Quantifying the loss mechanisms of nitrogen. Journal of Soil Water Conservation, 2002.

Dunn, et al. Assessing the effects of land use on temporal change in well water quality in a designated nitrate vulnerable zone. The Science of the Total Environment 265, 2001.

Duque, C., Müller, S., Sebok, E., Haider, K., and Engesgaard, P. (2016) Estimating groundwater discharge to surface waters using heat as a tracer in low flux environments: the role of thermal conductivity. Hydrol. Process., 30: 383–395. doi: 10.1002/hyp.10568.

Durant, N.D. and Myers, V.B., 2018. EPA’s approach to vadose zone monitoring at RCRA facilities. In Handbook of Vadose Zone Characterization & Monitoring (pp. 9-22). CRC Press.

Evans, T.A., D.R. Maidment. 1995 A spatial and statistical assessment of the vulnerability of Texas groundwater to nitrate contamination. CRWR online report 95–2. Centre for Research in Water Resources, The University of Texas at Austin

Flury, M.; Papritz, A. Bromide in the natural environment: Occurrence and toxicity. Journal of Environmental Quality 22(4): 747-758. 1993. 0047-2425. https://eurekamag.com/research/008/246/008246260.php

Gassman, P. W., Reyes, M. R., Green, C. H., & Arnold, J. G. (2007). The soil and water assessment tool: historical development, applications, and future research directions. Transactions of the ASABE, 50(4), 1211-1250.

Gassman, P. W., Williams, J. R., Benson, V. W., Izaurralde, R. C., Hauck, L. M., Jones, C. A., Atwood, J. D., Kiniry, J., & Flowers, J. D. (2005). Historical development and applications of the epic and apex models. Working Paper 05-WP 397. Ames, Iowa: Iowa State University, Center for Agricultural and Rural Development.

Halloran, L. J., Rau, G. C., & Andersen, M. S. (2016). Heat as a tracer to quantify processes and properties in the vadose zone: A review. Earth-Science Reviews, 159, 358-373.

Harter T. and H. Morel-Seytoux (2013). Peer Review of the IWFM, MODFLOW and HGS Model Codes: Potential for Water Management Applications in California’s Central Valley and Other Irrigated Groundwater Basins. Final Report, California Water and Environmental Modeling Forum, August 2013, Sacramento

Harter et. al. 2017, Source area management practices as remediation tool to address groundwater nitrate pollution in drinking supply wells. Journal of Contaminant Hydrology. DOI:10.1016/j.jconhyd.2019.103521.

Heatwole, K. K., & McCray, J. E. (2007). Modeling potential vadose-zone transport of nitrogen from onsite wastewater systems at the development scale. Journal of Contaminant Hydrology, 91(1-2), 184-201.

Hendrickx, J. M., & Flury, M. (2001). Uniform and preferential flow mechanisms in the vadose zone. *Conceptual models of flow and transport in the fractured vadose zone*, 149-187.

Holden, P.A., N. Fierer, VADOSE ZONE | Microbial Ecology, Encyclopedia of Soils in the Environment, Elsevier, 2005, Pages 216-224, ISBN 9780123485304, https://doi.org/10.1016/B0-12-348530-4/00172-7.

Hoffman, Iael Raij-, Kenneth Miller, George Paul, Yohannes Yimam, Sushant Mehan, John Dickey, Thomas Harter, Isaya Kisekka. Modeling water and nitrogen dynamics from processing tomatoes under different management scenarios in the San Joaquin Valley of California. Journal of Hydrology: Regional Studies, Volume 43, 2022. 101195, ISSN 2214-5818, https://doi.org/10.1016/j.ejrh.2022.101195.

Hoogenboom, G., C.H. Porter, K.J. Boote, V. Shelia, P.W. Wilkens, U. Singh, J.W. White, S. Asseng, J.I. Lizaso, L.P. Moreno, W. Pavan, R. Ogoshi, L.A. Hunt, G.Y. Tsuji, and J.W. Jones. 2019. The DSSAT crop modeling ecosystem. In: p.173-216 [K.J. Boote, editor] Advances in Crop Modeling for a Sustainable Agriculture. Burleigh Dodds Science Publishing, Cambridge, United Kingdom (http://dx.doi.org/10.19103/AS.2019.0061.10)

International Association of Hydrogeologists (IAH/AIH), 2023.

Jones, J.W., G. Hoogenboom, C.H. Porter, K.J. Boote, W.D. Batchelor, L.A. Hunt, P.W. Wilkens, U. Singh, A.J. Gijsman, and J.T. Ritchie. 2003. The DSSAT cropping system model. European Journal of Agronomy 18:235-265. (https://doi.org/10.1016/S1161-0301(02)00107-7)

Kim, N. W., Chung, I. M., Won, Y. S., & Arnold, J. G. (2008). Development and application of the integrated SWAT–MODFLOW model. Journal of hydrology, 356(1-2), 1-16.

Lai, S.-H. and Jurinak, J.J. (1971), Numerical Approximation of Cation Exchange in Miscible Displacement through Soil Columns. Soil Science Society of America Journal, 35: 894-899. https://doi.org/10.2136/sssaj1971.03615995003500060017x

Latham, J., Cumani, R., Rosati, I., & Bloise, M. (2014). Global land cover share (GLC-SHARE) database beta-release version 1.0-2014. FAO: Rome, Italy, 29.

Levy, B. S., & Chambers, R. M. (1987). Bromide as a conservative tracer for soil-water studies. Hydrological Processes, 1, 385–389

Meisinger, et al. 2002. Principles for managing nitrogen leaching. Journal of Soil and Water Conservation v57.

Raij-Hoffman, I., Jacques, D. and Lazarovitch, N., 2020. Suction cup system-dependent variable boundary condition: Transient water flow and multicomponent solute transport. Vadose Zone Journal, 19(1), p.e20030.

Ransom, et al. A hybrid machine learning model to predict and visualize nitrate concentration throughout the Central Valley aquifer, California, USA. Science of the Total Environment 2017.

Ritchie, J.T., 1998. Soil water balance and plant water stress. Understanding options for agricultural production, pp.41-54.

Rimon, Y., Dahan, O., Nativ, R., Geyer, S., 2007. Water percolation through the deep vadose zone and groundwater recharge: Preliminary results based on a new vadose zone monitoring system. Water Resour. Res. 43, 1–12.

Rojas Fabro, Annette Yabel, et al. Spatial Distribution of Nitrate Health Risk Associated with Groundwater Use as Drinking Water in Merida, Mexico. Applied Geography, vol. 65, 2015, pp. 49–57.

Sanden, Blake. 2007. Fall irrigation management in drought year for almonds, pistachios, and citrus. September Kern Soil and Water Newsletter, Univ. CA Coop. Ext, Kern County. 8 pp.

Shrestha, S., Semkuyu, D. J., & Pandey, V. P. (2016). Assessment of groundwater vulnerability and risk to pollution in Kathmandu Valley, Nepal. Science of the Total Environment, 556, 23-35.

Simunek, J., Van Genuchten, M. T., & Sejna, M. (2005). The HYDRUS-1D software package for simulating the one-dimensional movement of water, heat, and multiple solutes in variably-saturated media. University of California-Riverside Research Reports, 3, 1-240.

Singh, G., Kaur, G., Williard, K., Schoonover, J. and Kang, J. (2018), Monitoring of Water and Solute Transport in the Vadose Zone: A Review. Vadose Zone Journal, 17: 1-23 160058. https://doi.org/10.2136/vzj2016.07.0058

Slater, L., Binley, A. M., Daily, W., & Johnson, R. (2000). Cross-hole electrical imaging of a controlled saline tracer injection. *Journal of applied geophysics*, *44*(2-3), 85-102.

Sosebee Jr, J. B., Geiszler, P. C., Winegardner, D. L., & Fisher, C. R. (1983). Contamination of groundwater samples with poly (vinyl chloride) adhesives and poly (vinyl chloride) primer from monitor wells. In Symposium on Hazardous and Industrial Solid Waste Testing (Vol. 2, pp. 38-50).

State Water Resource Control Board, 2021. Communities that Rely on A Contaminated Groundwater Source for Drinking Water. California Water Boards.

The Department of Water Resources (DWR) Groundwater Information Center Interactive Map Application (GICIMA), 2023.

Thermo Fisher Scientific Inc., 2008.

Turkeltaub, T., Kurtzman, D., & Dahan, O. (2016). Real-time monitoring of nitrate transport in the deep vadose zone under a crop field – implications for groundwater protection. Hydrology and Earth System Sciences, 20(8), 3099-3108. doi:https://doi.org/10.5194/hess-20-3099-2016.

Twarakavi, N. K. C., Šimůnek, J., & Seo, S. (2008). Evaluating interactions between groundwater and vadose zone using the HYDRUS-based flow package for MODFLOW. Vadose Zone Journal, 7(2), 757-768.

USDA Soil Survey Staff. 1999. Soil taxonomy: A basic system of soil classification for making and interpreting soil surveys. 2nd edition. Natural Resources Conservation Service. U.S. Department of Agriculture Handbook 436.

U.S. EPA. 1978. Hazardous Waste: Proposed guidelines and regulations and proposal on identification and listings. Federal Regitser, v. 43, pp. 58986, 59005.

van Genuchten, M.Th. 1980. A closed-form equation for predicting the hydraulic conductivity of unsaturated soils. Soil Sci. Soc. Am. J. 44:892–898.

Venkatesan, G., Subramani, T., Karunanidhi, D., Sathya, U., & Li, P. (2021). Impact of precipitation disparity on groundwater fluctuation in a semi-arid region (Vellore district) of southern India using geospatial techniques. Environmental Science and Pollution Research, 28, 18539-18551.

Weihermüller, L., Kasteel, R., Vanderborght, J., Pütz, T., & Vereecken, H. (2005). Soil water extraction with a suction cup: Results of numerical simulations. Vadose Zone Journal, 4(4), 899-907.

Weissman G, Bel G, Ben-Gal A, et al. Increased irrigation water salinity enhances nitrate transport to deep unsaturated soil. Vadose Zone J. 2020;19:e20041.

Wick et al. 2012. Groundwater nitrate contamination: Factors and indicators. Journal of Environmental Management.

Zamora, D. S., Jose, S., Jones, J. W., and Cropper, W. P. Jr. (2009). Modeling cotton production response to shading in a pecan alleycropping system using CROPGRO. *Agrofor. Syst.* 76, 423–435. doi: 10.1007/s10457-008-9166-x